

# Floral organ- and temperature-dependent regulation of anthocyanin biosynthesis in *Cymbidium* hybrid flowers

著者	Nakatsuka Takashi, Suzuki Tomohiro, Harada Kenji, Kobayashi Yuki, Dohra Hideo, Ohno Hajime
journal or publication title	Plant Science
volume	287
page range	110173
year	2019-10
出版者	Elsevier
権利	(C) 2019. This manuscript version is made available under the CC-BY-NC-ND 4.0 license <a href="http://creativecommons.org/licenses/by-nc-nd/4.0/">http://creativecommons.org/licenses/by-nc-nd/4.0/</a>
URL	<a href="http://hdl.handle.net/10297/00026724">http://hdl.handle.net/10297/00026724</a>

doi: 10.1016/j.plantsci.2019.110173

1 **Floral organ- and temperature-dependent regulation of anthocyanin biosynthesis in**  
2 ***Cymbidium* hybrid flowers**

3

4 Takashi Nakatsuka <sup>1,2, \*</sup>, Tomohiro Suzuki <sup>3, 4</sup>, Kenji Harada <sup>1</sup>, Yuki Kobayashi <sup>1</sup>, Hideo  
5 Dohra <sup>3</sup>, Hajime Ohno <sup>1,2</sup>

6

7 <sup>1</sup> Faculty of Agriculture, Shizuoka University, Shizuoka 422-8529 Japan

8 <sup>2</sup> College of Agriculture, Academic Institute, Shizuoka University, Shizuoka 422-8529  
9 Japan

10 <sup>3</sup> Research Institute of Green Science and Technology, Shizuoka University, Shizuoka  
11 422-8529 Japan

12 <sup>4</sup> Center for Bioscience Research and Education, Utsunomiya University, Utsunomiya  
13 321-8508 Japan

14

15 **\* Corresponding author**

16 Takashi Nakatsuka, Ph. D.

17 College of Agriculture, Academic Institute, Shizuoka University, 836 Ohya Suruga-ku  
18 Shizuoka, 422-8529 Japan

19 Tel & Fax: +81-54-238-4353

20 e-mail: [nakatsuka.takashi@shizuoka.ac.jp](mailto:nakatsuka.takashi@shizuoka.ac.jp)

21

22 **Abstract**

23 Anthocyanins are responsible for red, purple, and pink pigmentation of flowers in  
24 *Cymbidium* hybrids. Although anthocyanin content in all floral organs increases with  
25 flower development, they increase markedly in the tepals compared with the labella or

26 columns. Using next-generation sequencing technology, we identified three anthocyanin  
27 biosynthesis regulatory genes, *CyMYB1*, *CybHLH1*, and *CybHLH2*, from *Cymbidium*  
28 ‘Mystique’. Yeast two-hybrid analysis showed that the CyMYB1 protein can form a  
29 heterodimer with either CybHLH1 or CybHLH2. In the tepals, the expression level of  
30 *CyMYB1* increased as the flower developed, whereas the high expression level of  
31 *CyMYB1* was detected at the early flower developmental stages in the labella and columns,  
32 remaining constant until increasing at the late developmental stage. These expression  
33 profiles of *CyMYB1* positively correlated with the profiles of anthocyanin accumulation  
34 in the tepals. When *Cymbidium* Sazanami ‘Champion’ was grown at 30°C/25°C, reduced  
35 anthocyanin levels were observed, specifically in the tepals, compared with those in  
36 flowers grown at 20°C/15°C. The transcription of *CyMYB1* in the tepals was suppressed  
37 at high temperatures, and the expressions of *CyDFR* and *CyANS* were also synchronously  
38 suppressed. This study revealed that *CyMYB1* activates the transcription of *CyDFR* and  
39 *CyANS* and regulates the temporal- and temperature-dependent anthocyanin  
40 accumulation in *Cymbidium* tepals.

#### 41 **Keywords**

42 Anthocyanin, high temperature, RNA-Seq, R2R3-MYB

43

#### 44 **Abbreviations**

45 **3GT** anthocyanidin 3-*O*-glucosyltransferase,

46 **3RT** anthocyanidin 3-*O*-glucoside rhamnosyltransferase

47 **ANS** anthocyanidin synthase

48 **bHLH** basic Helix-Loop-Helix

49 **CHS** chalcone synthase

50 **CHI** chalcone isomerase

- 51 **Cy3G** cyanidin 3-*O*-glucoside
- 52 **Cy3R** cyanidin 3-*O*-malonylglucoside
- 53 **Cy3R** cyanidin 3-*O*-rutinoside
- 54 **DFR** dihydroflavonol 4-reductase
- 55 **EFP** enhancer of flavonoid production
- 56 **F3H** flavanone 3-hydroxylase
- 57 **F3'H** flavonoid 3'-hydroxylase
- 58 **FLS** flavonol synthase
- 59 **HPLC** high performance liquid chromatography
- 60 **MalT** anthocyanin:malonyl-CoA acyltransferase
- 61 **Pe3R** peonidin 3-*O*- rutinoside
- 62 **qPCR** quantitative polymerase chain reaction
- 63 **WDR** WD40 repeat

64

## 65 **1. Introduction**

66 *Cymbidium* spp. is one of the most commercially popular orchids, along with  
 67 *Phalaenopsis* spp., and is utilized as a cut flower or potted plant in floriculture worldwide.  
 68 The genus *Cymbidium* is a member of the Orchidaceae family containing approximately  
 69 700 genera, and consists of 44 species, which are distributed across tropical and  
 70 subtropical Asia and northern Australia (Arditti, 1992). *Cymbidium* has been grown as a  
 71 cultivated plant for over one hundred years, and remains, to the present day, one of the  
 72 most important orchids in commerce.

73 *Cymbidium* flowers are composed of four different organs of different forms,  
 74 including three petal-like sepals, two lateral petals, one labellum, and one column organ.  
 75 The morphogenetic characters of the petal-like sepals are so similar to those of the lateral

76 petals that both are called tepals, whereas the structure of the labellum organ is  
77 significantly different from that of the other flower organs (Figs. 1A and B).

78 *Cymbidium* hybrid cultivars exhibit a range of flower colors, including white,  
79 pink, red, purple, yellow, and green [1]. Of these, anthocyanin accumulation is  
80 responsible for pink, red, and purple flower colorations, whereas carotenoid and  
81 chlorophyll accumulations are responsible for yellow and green colorations, respectively,  
82 in the floral organs of *Cymbidium* [2]. Cyanidin 3-*O*-glucoside, cyanidin 3-*O*-rutinoside,  
83 and cyanidin 3-*O*-(6"-malonylglucoside) have been identified as the major anthocyanins  
84 in cyanic *Cymbidium* cultivars [1].

85 Anthocyanin biosynthesis has been well studied in model plants, including  
86 *Arabidopsis thaliana*, *Zea mays*, *Antirrhinum majus*, and *Petunia hybrida* [3, 4]. Several  
87 studies have been reported the molecular biology of flower pigmentation in other genera  
88 of the Orchidaceae family, namely *Oncidium* [5-7] and *Phalaenopsis* [8]. However, there  
89 have been few reports of differential expression analysis of anthocyanin biosynthetic  
90 genes in *Cymbidium* hybrids. The dihydroflavonol 4-reductase (DFR)-encoding gene was  
91 isolated from a *Cymbidium* hybrid and shown to be unable to reduce dihydromyricetin to  
92 leucodelphinidin [9]. The genes encoding chalcone synthase (CHS), flavonol synthase  
93 (FLS), flavonoid 3'-hydroxylase (F3'H), and anthocyanidin synthase (ANS) have also  
94 been identified from a *Cymbidium* hybrid [10]. However, in the putative anthocyanin  
95 biosynthetic pathway in *Cymbidium* floral organs illustrated in Supplementary Fig. S1,  
96 the genes encoding chalcone isomerase (CHI), flavanone 3-hydroxylase (F3H),  
97 anthocyanidin 3-*O*-glucosyltransferase (3GT), anthocyanidin 3-*O*-glucoside  
98 rhamnosyltransferase (3RT), and anthocyanin: malonyl-CoA acyltransferase (MalT) have  
99 still to be isolated and identified.

100 It is known that the regulation of anthocyanin biosynthesis is controlled by the MYB-

101 bHLH-WDR complex composed of three proteins, namely the R2R3-MYB, the basic  
102 Helix-Loop-Helix (bHLH), and the WD40 repeat (WDR) proteins [11, 12]. In the  
103 Orchidaceae family, it has also been reported that the floral pigmentation of *Oncidium* is  
104 regulated by *OsMYB1* [5, 6]. The flower coloration and color patterning of *Phalaenopsis*  
105 are also regulated by three R2R3-MYB genes, namely *PeMYB2*, *PeMYB11*, and  
106 *PeMYB12* [8]. In a *Dendrobium* hybrid, *DhMYB2* and *DhbHLH1* are responsible for  
107 regulating anthocyanin biosynthesis [13]. When the *Leaf color (Lc, bHLH)* and *Colorless*  
108 *1 (C1, MYB)* genes from *Z. mays* were transiently expressed in white-flowered petals of  
109 the *Cymbidium* hybrid ‘Jung Frau dos Pueblos’, anthocyanin-producing cells were  
110 observed [14]. Therefore, the regulation of anthocyanin accumulation in *Cymbidium*  
111 petals could be controlled by the MYB/bHLH complex. However, although the regulatory  
112 genes of anthocyanin biosynthesis have been identified in other Orchidaceae members,  
113 no research has yet been reported in *Cymbidium*. Transcriptome sequence data of 11  
114 orchid species are available at OrchidBase [15, 16]. The genome sequence of  
115 *Phalaenopsis equestris* has also been published [17], while the molecular biology  
116 characteristics of *Cymbidium ensifolium* have also been studied in terms of transcriptome  
117 [18-20] and proteome [21]. *C. ensifolium* is one of the parent species involved in the  
118 breeding of *Cymbidium* hybrids, but anthocyanin accumulation was not observed in its  
119 tepal organs. Therefore, there is no molecular genetic resource available for analysis of  
120 the genes regulating flower pigmentation in *Cymbidium* hybrid cultivars. Expressed-  
121 sequence tag sequencing using next-generation sequencing has been utilized to identify  
122 several genes related to important floral traits of horticultural plants where genome  
123 information is lacking [22-24].

124 It has long been known that growth temperature conditions affect anthocyanin  
125 accumulation levels in the petals of petunia [25, 26], chrysanthemum [27], aster [28], rose

126 [29], and lily [30], in the fruits of apple [31] and grape [32], and in the seedlings of  
127 *Arabidopsis* [33] and maize [34]. Generally, moderate to low temperatures increase  
128 anthocyanin accumulation, whereas high temperatures decrease it [35]. *Cymbidium* plants  
129 usually bloom during the winter in Japan. Therefore, the flower color intensity of  
130 *Cymbidium* may also be affected by the growth temperature, but this has not yet been  
131 studied.

132 Here, we identified the anthocyanin biosynthetic regulatory gene *CyMYB1* from a  
133 *Cymbidium* hybrid using next-generation sequencing and revealed that the expression of  
134 *CyMYB1* was suppressed at high temperatures, leading to reduced anthocyanin  
135 accumulation in the tepals of *Cymbidium*.

136

## 137 **2. Materials and Methods**

### 138 **2.1. Plant materials**

139 Plants of the *Cymbidium* hybrid ‘Mystique’ were grown in a field of Shizuoka  
140 University, Japan. Three floral organs, namely the tepal, the labellum, and the column  
141 (Fig. 1A), were collected, snap-frozen immediately in liquid nitrogen, and stored  
142 separately at  $-80^{\circ}\text{C}$  until they were used. Flowers were collected at four floral  
143 development stages as follows: stage 1 (S1), perianth height, 15 to 20 mm; S2, perianth  
144 height, 20 to 25 mm; S3, perianth height, 25 to 30 mm; and S4, anthesis (Fig. 1B).

145 *Cymbidium* Sazanami ‘Champion’ was also used to investigate the effects of the  
146 growing temperature on flavonoid accumulation and expression of the corresponding  
147 biosynthetic genes. The flower pigmentation of this cultivar responded more to the growth  
148 temperature than did ‘Mystique’. *Cymbidium* Sazanami ‘Champion’ plants with S2-  
149 flower buds growing in pots were transferred to two different growth chambers, namely  
150 at low- ( $20^{\circ}\text{C}/15^{\circ}\text{C}$  day/night) and high-temperature conditions ( $30^{\circ}\text{C}/25^{\circ}\text{C}$ ), under a 12-

151 h photoperiod, with light supplied by a high-pressure sodium lamp.

152

## 153 **2.2 Flavonoid analysis**

154 A sample (100 mg fresh weight) of each organ was powdered using liquid  
155 nitrogen and then extracted in 1 mL of extraction solution containing 40% (v/v) methanol  
156 and 10% (v/v) acetic acid, for 24 h at 4°C. The extract was then filtered by passage  
157 through a 0.22- $\mu$ m PTFE syringe filter (Osaka Chemical, Osaka, Japan). Anthocyanin and  
158 flavonol analyses were carried out by the Agilent Infinity 1290 HPLC system (Agilent  
159 Technologies, Santa Clara, CA, USA) with an Agilent 1200 Diode-Array Detector SL  
160 (Agilent Technologies), and a reversed-phase column ZORBAX SB-C18 (2.1  $\times$  50 mm,  
161 1.8  $\mu$ m). Two solvents, solvent A (1.5% [v/v] phosphoric acid) and solvent B (1.5% [v/v]  
162 phosphoric acid containing 20% (v/v) acetic acid and 25% (v/v) acetonitrile), were used  
163 for elution at 40°C at a flow rate of 1.0 mL min<sup>-1</sup>. The elution was performed with 10%  
164 solvent A for 1 min, and then increasing to 60% solvent A for 8 min using gradient.  
165 Anthocyanins and flavonols were monitored as absorbance at 525 and 360 nm,  
166 respectively. The anthocyanin concentration was calculated using standards (cyanidin 3-  
167 *O*-glucoside and cyanidin 3-*O*-rhamnoside; Extrasynthese, Lyon, France). Since a  
168 standard of cyanidin 3-*O*-malonyglucoside was not commercially available, the  
169 concentration of this molecule was calculated using a standard curve of cyanidin-3-*O*-  
170 glucoside. The flavonol concentration was calculated from area of all peaks detected at  
171 360 nm.

172

## 173 **2.3. Construction of a cDNA library from *Cymbidium labella***

174 Total RNAs were isolated from labella of *Cymbidium* 'Mystique' using RNAiso Plus  
175 (Takara Bio, Shiga, Japan) with Fruit-mate for RNA Purification (Takara Bio), and then



176 treated with DNase I to remove any remaining genomic DNA. The cDNA library was  
177 synthesized using the SureSelect Strand-Specific RNA Library Prep for Illumina  
178 Multiplexed Sequencing (Agilent Technologies) according to the manufacturer's  
179 instructions. The library obtained was adjusted to a concentration of 20 pM, and  
180 sequencing was performed with  $2 \times 75$ -bp paired-end reads on the Illumina MiSeq Next-  
181 Generation Sequencer (Illumina). The adapters and other low-quality reads were removed  
182 from the raw sequence data using cutadapt (version 1.8.1) [36] to trim low-quality ends  
183 (<QV30), the 76th nucleotides, and adapter sequences, and to discard reads shorter than  
184 50 bp, and the clean reads were assembled using Trinity software version r20140413p1  
185 [37]. The contigs obtained were defined as unigenes after removing any redundancy.  
186 These unigenes were submitted to the *Arabidopsis* protein database TAIR10 (The  
187 Arabidopsis Information Resource [TAIR]) for homology and annotation comparison by  
188 the BLASTX algorithm and by InterPro. The Blast2GO program [38] was used in GO  
189 annotation and functional classification.

190

#### 191 **2.4. Isolation of anthocyanin biosynthesis genes from *Cymbidium***

192 The putative open reading frames (ORFs) of the *Cymbidium* anthocyanin  
193 biosynthesis genes were expected to be obtained from the *Cymbidium* cDNA library.  
194 However, many contigs did not contain the complete coding region. Therefore, we used  
195 the rapid amplification of cDNA ends technology to obtain full-length cDNA sequences  
196 using the GeneRacer Kit (Invitrogen, by Thermo Fisher Scientific, Carlsbad, CA, USA).  
197 The ORF sequences were amplified using Takara *Ex-Taq* polymerase (Takara Bio), and  
198 the primer sets are shown in Supplementary Table S1. The thermal cycler program was  
199 set as follows: 94°C for 2 min, then 35 cycles of 94°C for 20 s, 60°C for 40 s, and 72°C  
200 for 2 min, and a last step at 72°C for 10 min. The amplified fragments were purified using

201 Wizard SV gel and PCR Clean-Up System (Promega, Madison, WI, USA), and were  
202 subcloned into the pGEM-Teasy vector system (Promega). The sequences of all  
203 constructs were confirmed by DNA sequencing (Fasmac, Kanagawa, Japan). For  
204 phylogenetic analysis of the CyMYBs, the deduced amino acid sequences of the R2R3  
205 domain of CyMYBs were aligned with R2R3-MYBs from other species using ClustalW  
206 [39]. A phylogenetic tree was constructed by Molecular Evolutionary Genetics Analysis  
207 version 6.0 (MEGA6) using the neighbor-joining method with 1,000 bootstrapping data  
208 sets [40].

209

## 210 ***2.5. Gene expression analysis***

211 Total RNAs were isolated from each floral organ of *Cymbidium* 'Mystique' at  
212 the different developmental stages described above. The elimination of genomic DNA  
213 and cDNA synthesis were carried out using the PrimeScript RT Reagent Kit with gDNA  
214 Eraser (Takara Bio). Quantitative real time PCR (qPCR) analysis of each gene was  
215 performed with Thermal Cycler Dice Real Time System (TP850; Takara Bio) using the  
216 KAPA SYBR FAST qPCR Master Mix kit (KAPA Biosystems, Wilmington, MA, USA).  
217 Briefly, the reaction mixture (10  $\mu$ L) consisted of 1 $\times$  Master Mix, 0.2  $\mu$ M each primer,  
218 and 1  $\mu$ L template cDNA. The cycling conditions were as follows: 95°C for 20 s, followed  
219 by 40 cycles of 95°C for 1 s and 60°C for 20 s. The specificity of each amplification  
220 reaction was checked by the addition of a dissociation analysis step after the cycle  
221 reaction. The data were analyzed by second derivative maximum methods using the  
222 Thermal Cycler Dice Real Time System II software version 5.00 (Takara Bio). The  
223 transcript level of each gene was calculated relative to that of the *Cymbidium* actin-  
224 encoding *CyACT1* (LC424204) as a reference gene. The qPCR analyses were performed  
225 with six biological replicates. The sequences of all primers used in the qPCR analysis are

226 listed in supplementary Table S2.

227

## 228 ***2.6. Protein–protein interaction between CyMYB1 and CybHLHs***

229 To investigate the interactions among the CyMYB1, CybHLH1, and CybHLH2  
230 proteins, we employed the yeast two-hybrid analysis using a Matchmaker Two-Hybrid  
231 System 3 (Clontech, Takara Bio, Otsu, Shiga, Japan). The coding regions of *CyMYB1*,  
232 *CybHLH1*, and *CybHLH2* were cloned into either the pGAD-T7 (GAL4 activation  
233 domain) or pGBK-T7 (GAL4 DNA-binding domain) vector. All constructs were  
234 transformed into *Saccharomyces cerevisiae* AH109 (Clontech, Takara Bio). The  
235 transformed yeast cells were grown on SD selective medium without leucine (–Leu) and  
236 tryptophan (–Trp) at 30°C for 3 days. The survival test for each transformed yeast culture  
237 was performed on selective quadruple-dropout medium (–Leu, –Trp, histidine [–His],  
238 and adenine [–Ade]) supplemented with 15 mM 3-amino-1,2,4-triazole (3-AT) at 30°C  
239 for 3 days.

240

## 241 ***2.7. Statistical analysis***

242 Data are presented as mean ± SE. Statistical comparisons were carried out using the  
243 Student’s *t*-test.

244

## 245 **3. Results**

### 246 ***3.1. Isolation of anthocyanin biosynthesis-related genes using next-generation*** 247 ***sequencing***

248 To construct a unigene catalog of *Cymbidium* ‘Mystique’ labella, we performed  
249 RNA-Seq using 75-bp paired-end reads in Illumina MiSeq. After quality filtering and  
250 read cleaning, we obtained approximately 16 million sequencing raw reads, from which

251 59,000 contigs were assembled with an average sequence length of 922 bp.

252 Based on either homology search by BLAST or domain search by InterPro, 15  
253 contigs of the R2R3-MYB transcription factor were found in the *Cymbidium* ‘Mystique’  
254 flower cDNA contigs. They were classified into each subfamily by phylogenetic analysis  
255 (Fig. 2). The deduced amino acid sequence of *CyMYB1* (DDBJ accession number  
256 LC422758) exhibited 70.6% and 71.2% identities with those of the *Oncidium* hybrid  
257 *MYB1* and *Arabidopsis thaliana* *TRANSPARENT TESTA 2 (TT2)*, respectively, which  
258 have been recognized to be anthocyanin biosynthesis regulators, and were categorized  
259 into the *C1* subfamily. In addition, *CyMYB1* was categorized into a clade including  
260 anthocyanin biosynthesis-related R2R3-MYBs from other members of the Orchidaceae  
261 (Fig. 2). The bHLH interaction motif [D/E]Lx2[R/K]x3Lx6Lx3R [41] was well  
262 conserved within the R3 repeat domain of *CyMYB1* (76<sup>th</sup>–95<sup>th</sup> residues).

263 Two *bHLH* orthologs, *CybHLH1* (LC422759) and *CybHLH2* (LC422760), were also  
264 found among the *Cymbidium* flower cDNA contigs (Supplementary Fig. S2). The  
265 deduced amino acid sequence of *CybHLH1* exhibited 76.9% identity with that of  
266 *CybHLH2*. Moreover, *CybHLH1* and *CybHLH2* exhibited 47.3% and 47.4% identities,  
267 respectively, with a *Dendrobium* hybrid *DhbHLH1* (AQS79853, [13]). They also  
268 exhibited 49.1% and 49.0% identities with the *Lilium* hybrid bHLH (BAE20057, [42]).  
269 *CybHLH1* and *CybHLH2* were classified into a clade that included the *Lilium* hybrid  
270 bHLH1, which was different from the clade that contained the other orchid bHLHs  
271 (Supplementary Fig. S2). We attempted to identify an anthocyanin biosynthesis-related  
272 WDR *Arabidopsis* TTG1 but could identify no WDR ortholog from the *Cymbidium*  
273 flower cDNA contigs (data not shown).

274 In addition, we were successful in identifying anthocyanin biosynthesis genes,  
275 including *CyCHI* (LC422751), *CyCHI2/EFP* (LC422750), *CyF3H* (LC422752),

276 *CyF3'H1* (LC422753), *CyF3'H2* (LC422754), *Cy3GT* (LC422755), *Cy3RT* (LC422756),  
277 and *CyMalT* (LC4227557) from *Cymbidium* (Supplementary Figs. S3–S7). Of these, the  
278 predicted amino acid sequences of the proteins encoded by two *F3'H* genes, *CyF3'H1* and  
279 *CyF3'H2*, exhibited low amino acid sequence similarity with the protein encoded by  
280 *ChF3'H* (KM186178), which had been previously reported by Wang et al. [10]. The  
281 deduced amino acid sequence of *CyF3'H1* exhibited 57.7% identity with that of *CyF3'H2*,  
282 and the sequences of *CyF3'H1* and *CyF3'H2* exhibited 51.9% and 54.7% identities,  
283 respectively, with the amino acid sequence of *ChF3'H* (Supplementary Fig. S5). These  
284 results suggest that sequence diversity seems to exist within the *F3'H* gene in *Cymbidium*  
285 hybrids.

286

### 287 **3.2. Protein–protein interaction between *CyMYB1* and *CybHLHs***

288 To investigate whether *CyMYB1* interacts with either *CybHLH1* or *CybHLH2*,  
289 we employed a GAL4-based yeast two-hybrid system (Fig. 3). All yeasts harboring GAL4  
290 DNA-binding-domain-fused *CyMYB1* grew in the quadruple-dropout medium,  
291 suggesting false positive results. The yeasts harboring the combination of *CyMYB1* and  
292 either *CybHLH1* or *CybHLH2* survived on quadruple-dropout medium, and no difference  
293 in the growth speed was observed in either combination of *CyMYB1* and either  
294 *CybHLH1* or *CybHLH2*. The yeasts harboring the combination of *CybHLH1* and  
295 *CybHLH2* also showed low survival on quadruple-dropout medium, suggesting the  
296 formation of heterodimers or homodimers within/between *CybHLH1* and *CybHLH2*.  
297 These results support the hypothesis that *CyMYB1* and either *CybHLH1* or *CybHLH2*  
298 form a heterodimer, as reported for anthocyanin transcription factors from other plants  
299 [12].

300

301 **3.3. Temporal changes of flavonoid accumulation and flavonoid biosynthetic gene**  
302 **expressions in *Cymbidium* ‘Mystique’ tepals**

303 The anthocyanin and flavonol concentrations in the tepals at different flower  
304 developmental stages were determined using HPLC. The major anthocyanins extracted  
305 from *Cymbidium* ‘Mystique’ flowers were three cyanidin derivatives, namely cyanidin 3-  
306 *O*-glucoside, cyanidin 3-*O*-rutinoside, and cyanidin 3-*O*-malonylglucoside, confirming  
307 the findings of Tatsuzawa et al. [1]. Total anthocyanin content per tepal increased to 21.8  
308 µg during flower development and was closely associated with the development of tepal  
309 pigmentation (Figs. 1A and 1C). The three anthocyanin components, including cyanidin  
310 3-*O*-glucoside, cyanidin 3-*O*-rutinoside, and cyanidin-3-*O*-malonylglucoside, were  
311 present in nearly equal ratios, and no change in the amounts occurred during floral  
312 development. The peak at retention time 3.45 min corresponded to the major flavonol  
313 compound and represented approximately 60% of the total flavonols in all organs during  
314 flower development (data not shown). However, because we could not identify the  
315 structure of this major compound, flavonol amount was shown by the peak area of  
316 chromatograms at 360 nm. In the tepals, the flavonol content at S4 increased to 1.9 times  
317 than that at S1 (Fig. 1D).

318 To investigate the expression profiles of putative flavonoid biosynthesis  
319 regulatory genes in the tepals during flower development in *Cymbidium* ‘Mystique’, we  
320 performed qPCR analysis (Fig. 4). The expression levels of *CyMYB1* increased in the  
321 tepals during floral development, with the maximum expression levels being achieved at  
322 the floral developmental stage 3 (S3). These temporal expression profiles closely  
323 correlated with those of anthocyanin accumulation in *Cymbidium* tepals (Fig. 1C).  
324 Conversely, *CybHLH1* and *CybHLH2* transcript abundance was constant from S1 flower  
325 developmental stage to stage 3 at which point they increased and decreased, respectively,

326 at stage 4 (Fig. 4). Therefore, neither *CybHLH1* nor *CybHLH2* exhibited the dynamic  
327 expression variation corresponding with the anthocyanin accumulation profiles in tepals  
328 as *CyMYBI* did.

329 In addition, we investigated the temporal expression profiles of the structural genes  
330 involved in anthocyanin and flavonol biosynthesis, including *CyCHS*, *CyCHI*, *CyEFP*,  
331 *CyF3H*, *CyFLS*, *CyF3'H1*, *CyF3'H2*, *CyDFR*, *CyANS*, *Cy3GT*, *Cy3RT*, and *CyMalT* in  
332 *Cymbidium* 'Mystique' tepals (Fig. 5). The temporal expression profiles of *CyCHS*,  
333 *CyF3H*, *CyF3'H2*, *CyDFR*, *CyANS* and *CyMalT* were relatively similar to the *CyMYBI*  
334 expression and anthocyanin accumulation profiles in the tepals (Figs. 1C, 4, and 5). These  
335 findings suggest that the expression of these anthocyanin biosynthesis genes is regulated  
336 by the *CyMYBI* transcription factor. Conversely, the high expression levels of *CyEFP* and  
337 *CyFLS* were detected in the tepals at all flower developmental stages (Fig. 5). The  
338 expression profiles of these two genes correlated well with that of *CybHLH2* and the  
339 flavonol accumulation profiles in the tepals (Figs. 1D and 5). The expression profiles of  
340 *3GT* and *3RT*, which encoded anthocyanin glycosyltransferases, did not correlate with  
341 either the anthocyanin or flavonol accumulation profile of any of the floral organs (Figs.  
342 1D and 5).

343

#### 344 ***3.4. Temporal changes of flavonoid accumulation and flavonoid biosynthetic gene*** 345 ***expressions in Cymbidium 'Mystique' labella***

346 The total anthocyanin content per labellum was similar to that in the tepals at the  
347 flower developmental stage 1 and increased to 7.4 µg/organ at flower development stage  
348 4 (Fig. 1C). Pigmentation was observed mainly at the upper parts of the labellum, with  
349 anthocyanin accumulating only slightly at the lower parts. The ratio of cyanidin 3-*O*-  
350 glucoside, cyanidin 3-*O*-rutinoside, and cyanidin-3-*O*-malonylglucoside was similar to

351 that in the tepals (Fig. 1C). Conversely, the flavonol content in the labellum at S1 was  
352 52.3% compared with that in the tepal. However, the flavonol content of the labellum at  
353 S4 had increased to 3.7 times than that at S1, being similar to the flavonol content of the  
354 tepals at S4 (Fig. 1D).

355 Furthermore, we investigated the expression profiles of flavonoid biosynthesis-  
356 related genes in the labellum during flower development in *Cymbidium* 'Mystique' (Figs.  
357 4 and 5). The abundance of *CyMYB1* transcripts was more-or-less constant from S1 to S3  
358 in the labellum, before significantly decreasing at S4 (Fig. 4). Similarly, the expression  
359 levels of *CybHLH1* in the labellum did not change throughout flower development.  
360 Moreover, the expression of *CybHLH2* in the labellum was strongly detected at S1, and  
361 then decreased during later floral development. These temporal expression profiles did  
362 not closely correlate with those of anthocyanin accumulation in the *Cymbidium* labellum  
363 (Fig. 1C). The structural genes *CyDFR*, *CyANS*, and *CyMalT* were expressed at a constant  
364 level in the labellum from S1 to S3, and then, the expression significantly decreased at  
365 S4, indicating that the expression profiles of these three genes resembled that of *CyMYB1*  
366 (Figs. 4 and 5). In contrast, the expression of *CyCHI*, *CyEFP*, *CyF3H*, *CyF3'H2*, and  
367 *CyFLS* decreased as the flower developed, indicating that the expression profiles were  
368 similar to that of *CybHLH2* (Figs. 4 and 5). The expression levels of *CyEFP*, *CyF3H*,  
369 *CyF3'H2*, and *CyFLS* in the labellum at flower development S1 were significantly greater  
370 than those in the tepals and columns.

371

### 372 ***3.5. Temporal changes of flavonoid accumulation and flavonoid biosynthetic gene*** 373 ***expressions in Cymbidium 'Mystique' columns***

374 Anthocyanin accumulation was under the detection level in the column at S1 (Fig.  
375 1C). Anthocyanin accumulation started at the base of the column at S2, with total



376 anthocyanin content per column reaching a peak of 6.2  $\mu\text{g}$  at S3. Peonidin 3-rutinoside,  
377 which was barely detectable in the tepals and labella, accumulated to 16.5% of the total  
378 anthocyanin content in the column (Fig. 1C). In addition, non-malonyl anthocyanins  
379 accounted for 79.2% of total column anthocyanins.

380 The temporal expression profiles of anthocyanin regulatory genes in the column  
381 were similar to those in the labellum than in the tepal (Fig. 4). The expression levels of  
382 *CyMYB1* and *CybHLH2* peaked at S2, and then decreased as the flower continued to  
383 develop. Conversely, *CybHLH1* was expressed constantly from S1 to S3, before  
384 increasing at S4 (Fig. 4). The regulatory gene expression profiles in the column did not  
385 correlate with either anthocyanin or flavonol accumulation profiles (Figs. 1C and 1D).  
386 The expressions of *CyDFR* and *CyANS* peaked at S2 in the labellum, before significantly  
387 decreasing at S4. The expression profiles of these two structural genes were similar to  
388 those of *CyMYB1* (Figs. 4 and 5). The maximum expression levels of *CyCHS*, *CyF3H*,  
389 and *CyF3'H2* in the column were significantly lower than those in either the tepals or  
390 labella.

391

### 392 **3.6. Suppression of anthocyanin accumulation induced by high temperature**

393 To investigate whether *CyMYB1* regulates anthocyanin biosynthesis in *Cymbidium*  
394 flowers, we carried out metabolite and gene expression analyses using *Cymbidium*  
395 flowers grown under different conditions. *Cymbidium* Sazanami 'Champion' with floral  
396 buds at stage S2 were grown at two different temperatures, namely low (20°C/15°C) or  
397 high (30°C/25°C). The low-temperature conditions in this study represented temperatures  
398 representative of those at which *Cymbidium* blooms in Japan. As shown in Fig. 6, the  
399 tepals of *Cymbidium* plants grown at high temperatures (B) were paler than those grown  
400 under low-temperature conditions (A). The anthocyanin concentration in tepals grown at

401 a high temperature decreased to 42.8% of that detected at a low temperature (Fig. 6C).  
402 However, no significant difference was observed in the anthocyanin concentration in  
403 either the labellum or column between high- and low-temperature conditions.  
404 Anthocyanin composition was also different between low- and high-temperature grown  
405 plants, with cyanidin 3-malonylglucoside (Cy3MG) concentration being reduced in the  
406 three floral organs (Fig. 6C). On the other hand, the flavonol concentrations in the tepals  
407 and columns were not affected by the growth temperature, although a significantly ( $P <$   
408 0.05) lower flavonol concentration was observed in the labellum grown under high-  
409 temperature conditions (Fig. 6D). These results show that anthocyanin concentration  
410 decreased in an organ-specific manner, i.e., only in tepals, when *Cymbidium* flowers were  
411 exposed to high temperatures.

412 We also investigated the expression of anthocyanin biosynthesis structural genes in  
413 the tepals and labella of flowering plants grown under different temperatures (Fig. 7).  
414 High expression levels of *FLS* were detected in the tepals and columns before the  
415 temperature treatment started (S2), following which there was no significant decrease in  
416 the *FLS* expression levels in either the tepals or labella grown under low- or high-  
417 temperature conditions (Fig. 7). This result correlated with changes in the flavonol  
418 concentration levels under both temperature conditions. The expression levels of  
419 anthocyanin biosynthesis genes, including *CyDFR* and *CyANS*, increased when  
420 *Cymbidium* was grown to stage S3 under low-temperature conditions, compared with the  
421 expression levels occurring pre-treatment at stage 2 (Fig. 7). However, the expression  
422 levels of *CyDFR* and *CyANS* did not increase under high-temperature conditions (Fig. 7).  
423 Similarly, the elevated expression of *CyMYB1* and *CybHLH2* observed under low-  
424 temperature conditions was not detected under high-temperature conditions in the tepals  
425 (Fig. 7). In the labellum of *Cymbidium* flowers grown under the high-temperature

426 conditions, the expression levels of *CyMYB1*, *CybHLH2*, *CyDFR*, and *CyANS* were  
427 suppressed compared with the labellum of flowers grown under low-temperature  
428 conditions. However, their transcript abundance in the labellum was higher than that in  
429 the tepal under high-temperature conditions. These results indicate that the expression of  
430 the regulatory genes *CyMYB1* and *CybHLH2* and the anthocyanin biosynthesis genes  
431 *CyDFR* and *CyANS* were suppressed at high temperatures, resulting in the reduced  
432 anthocyanin accumulation observed in the tepal organs (Fig. 6).

433

#### 434 **4. Discussion**

435 *Cymbidium* flowers exhibited different temporal profiles of anthocyanin  
436 accumulation among the tepal, labellum, and column organs (Figs. 1A and 1C). The  
437 anthocyanin concentration in all floral organs increased as the *Cymbidium* flowers  
438 developed. In tepals, anthocyanin accumulation increased 16.6-fold from flower  
439 development S1 to S4 (Fig. 1C), whereas in labella, anthocyanin accumulation increased  
440 5.8-fold during flower development. Anthocyanin accumulation was observed in the  
441 entire tepal, whereas it occurred in only the upper part of the labellum organs (Fig. 1A).  
442 On the other hand, the base of the column organ started to accumulate anthocyanins at S2.  
443 No difference in the flavonol accumulation profiles was observed among the three floral  
444 organs (Fig. 1D). Thus, we speculated that anthocyanin accumulation is strictly regulated  
445 in an organ-specific manner in *Cymbidium* flowers.

446 Some anthocyanin biosynthesis-related genes from *Cymbidium* had been reported  
447 previously [9, 10]. Wang et al. [10] reported the temporal and spatial expression profiles  
448 of some anthocyanin biosynthesis genes, *CHS*, *F3'H*, *DFR*, and *ANS*, in eight *Cymbidium*  
449 cultivars with different flower colors and color patterns. However, this paper did not  
450 investigate the integrated regulation of anthocyanin biosynthesis genes. The regulatory

451 mechanism of anthocyanin biosynthesis has been well studied in model plants, including  
452 *A. thaliana*, *Z. mays*, *A. majus*, and *P. × hybrida* [3, 4]. The R2R3-MYB and bHLH  
453 proteins that regulate anthocyanin biosynthesis have been extensively studied in many  
454 floricultural plants, including lily [43, 44], Japanese gentian [11, 45], and *Dendrobium*  
455 hybrid [13]. *C. ensifolium*, which is one of the parents used in the breeding of *Cymbidium*  
456 hybrids, is the source of several bio-resources including transcriptome [19, 20], proteome  
457 [21] and small-RNA transcriptome analyses [18]. However, anthocyanin accumulation is  
458 not observed in the *C. ensifolium* floral organs except for the tepals. Therefore, we carried  
459 out next-generation sequencing using the red-colored flower of the *Cymbidium* hybrid  
460 ‘Mystique’. In this study, we were successful in isolating almost all of the regulatory and  
461 structural genes involved in anthocyanin biosynthesis from the *Cymbidium* hybrid.  
462 Expressed-sequence tag sequencing using next-generation sequencing is important for  
463 conducting functional analysis, especially on horticultural plants where genome  
464 information is lacking. Next-generation sequencing technology has been utilized to  
465 identify several genes related to important floral traits of *Chrysanthemum × morifolium*  
466 [22], *Lilium* hybrid [23], and *Paeonia lactiflora* [24].

467 We isolated genes encoding 15 R2R3-MYB transcription factors from  
468 *Cymbidium* hybrid ‘Mystique’ floral cDNA contigs, with only *CyMYB1* being categorized  
469 into a clade belonging to the anthocyanin biosynthesis regulators reported in other orchids  
470 (Fig. 2). The deduced amino acid sequence of *CyMYB1* showed strong similarity with  
471 that of the anthocyanin biosynthesis-related R2R3-MYB transcription factors from other  
472 orchid species, including *Oncidium* OgMYB1 [5, 6], *Dendrobium* DhMYB2 [13], and  
473 *Phalaenopsis* PeMYBs [8]. Anthocyanin biosynthesis-related R2R3-MYBs are  
474 categorized into two subgroups, *C1* and *AN2*, based on the amino acid sequences [46].  
475 Most *R2R3-MYB* genes that regulate anthocyanin biosynthesis in flowers of eudicot

476 species and monocot *Lilium* species are in the AN2 subgroup [44, 46]. On the other hand,  
477 anthocyanin biosynthesis-related *R2R3-MYB* genes of most monocots, including  
478 members of the Poaceae and Orchidaceae, belong to the *CI* subgroup. CyMYB1 was also  
479 categorized into the same *CI* subgroup as anthocyanin regulatory factors from other  
480 Orchidaceae species (Fig. 2).

481 *Phalaenopsis* spp. has three anthocyanin biosynthesis-related *R2R3-MYB* genes,  
482 namely *PeMYB2*, *PeMYB11*, and *PeMYB12* [8]. Although they were grouped together in  
483 the same clade, *PeMYB2* showed strong activity with respect to anthocyanin biosynthesis,  
484 whereas *PeMYB11* and *PeMYB12* exhibited little activity. In the sepals/petals, *PeMYB2*,  
485 *PeMYB11*, and *PeMYB12* control full-red pigmentation, red spots, and venation patterns,  
486 respectively [8]. Moreover, *PeMYB11* controls the production of red spots in the callus,  
487 and *PeMYB12* is the major transcription factor controlling pigmentation in the central  
488 lobe of the labellum [8]. *Cymbidium* flowers also exhibit a wide range of intricate  
489 anthocyanin pigmentation patterns, including full tepal pigmentation, venation, spots,  
490 zones that lack pigmentation, and co-pigmentation (Figs. 1A and 6A) [47]. However, we  
491 could not find any *R2R3-MYB* homologs belonging to the *CI* subgroup except for  
492 CyMYB1 from the *Cymbidium* hybrid flower (Fig. 2). It is possible that some *CyMYB1*-  
493 like *R2R3-MYB* genes might be isolated from other *Cymbidium* cultivars with spotting or  
494 venation patterns. Albert et al. [14] reported that the combination of *CI* (*R2R3-MYB*) and  
495 *Lc* (*bHLH*) genes from *Z. mays* could induce anthocyanin pigmentation in the petals of  
496 the *Cymbidium* hybrid ‘Jung Frau dos Pueblos’, which is a commercial white-flowered  
497 cultivar. These results implied that *CI* and *Lc* orthologs might regulate anthocyanin  
498 biosynthesis in *Cymbidium* flowers. The phylogenetic analysis showed that CybHLH1  
499 and CybHLH2 were classified into the same clade as *Z. mays* *Lc* rather than other orchid  
500 bHLHs (Supplementary Fig. S2). These results suggested strongly that anthocyanin

501 accumulation in the *Cymbidium* flower is regulated by *CyMYB1* and *CybHHLH1/2*, which  
502 are maize *C1* and *Lc* orthologs, respectively. Moreover, yeast two-hybrid analysis showed  
503 that *CyMYB1* could interact with either *CybHHLH1* or *CybHHLH2* (Fig. 3). Therefore, this  
504 result also implied that the complex of *CyMYB1* and *CybHHLH1/2* regulates anthocyanin  
505 biosynthesis in the floral organs of *Cymbidium*.

506 The temporal and spatial profiles of the *CyMYB1* transcripts correlated closely with  
507 the profile of anthocyanin accumulation in the tepals (Fig. 1C and 4). On the other hand,  
508 neither *CybHHLH1* nor *CybHHLH2* showed such a dynamic variation in transcript  
509 abundance, which reflected the observed changes in anthocyanin and flavonoid  
510 accumulation (Fig. 1C and 4). Therefore, we speculated that *CyMYB1* is a key regulatory  
511 gene for anthocyanin biosynthesis in *Cymbidium* floral organs. In the kernel of *Z. mays*,  
512 MYB (C1/Pl) and bHLH (R1/B1) interact and activate the anthocyanin biosynthesis  
513 genes *CHS*, *CHI*, *F3H*, *DFR*, *ANS*, and *3GT* as a single unit [48]. In proanthocyanidin  
514 biosynthesis in *Arabidopsis* seeds, TT2, TT8, and TTG1 are involved in the MYB-bHLH-  
515 WDR complex, and they control the expression of the late biosynthesis genes, including  
516 *DFR*, *ANS*, *3GT*, leucoanthocyanidin reductase, and anthocyanidin reductase [48]. In  
517 anthocyanin synthesis in grapes, transcription of the *3GT* gene alone was regulated by  
518 two MYB genes, *VvMYBA1* and *VvMYBA2* [49, 50]. In a *Dendrobium* hybrid, *DhMYB2*  
519 and *DhbHHLH1* were synchronously expressed during petal development, and directly  
520 activated the transcription of *DhF3H*, *DhDFR*, and *DhANS* [13]. In an *Oncidium* hybrid,  
521 *OgMYB1* activated the transcription of the *OgCHI* and *OgDFR* genes, resulting in  
522 anthocyanin accumulation in normally unpigmented floral lip tissues [5, 6]. In the present  
523 study, of 12 anthocyanin and flavonol biosynthesis genes, the expression profiles of the  
524 *CyCHS*, *CyF3H*, *CyF3'H2*, *CyDFR*, *CyANS* and *CyMalT* genes were similar to that of  
525 *CyMYB1* in tepals (Figs. 4 and 5). In the labella, the temporal expression profiles of

526 *CyDFR*, *CyANS*, and *CyMalT* were also correlated with that of *CyMYB1* (Figs. 4 and 5).  
527 However, the expression profiles of structural genes encoding anthocyanin  
528 glycosyltransferases, including *Cy3GT* and *Cy3RT*, were not correlated with that of  
529 *CyMYB1* in the tepal or labellum organs (Fig. 4). Therefore, the expression of genes  
530 encoding these anthocyanin modification enzymes might not be controlled directly by  
531 *CyMYB1*. However, since both *Cy3RT* and *CyMalT* were candidate genes found among  
532 the *Cymbidium* floral cDNA contigs (Supplementary Figs. S6 and S7), it would be  
533 necessary to carry out further functional analysis on these genes. These results imply that  
534 *CyMYB1* interacted with either *CybHLH1* or *CybHLH2* and activated the transcription  
535 of *CyCHS*, *CyF3H*, and *CyF3'H* in the tepals as well as of *CyDFR*, *CyANS* and *CyMalT*  
536 in tepals and labella during flower development. However, we were not successful in  
537 activating anthocyanin biosynthesis by transient expression of *CyMYB1* in several organs  
538 of *Cymbidium* (data not shown). Moreover, no different observations of flower colors  
539 were made when *CyMYB1* was overexpressed in transgenic tobacco plants (data not  
540 shown). Therefore, we would remain to further study to reveal *CyMYB1* function in  
541 *Cymbidium* flowers.

542 The growth temperature is one of the main environmental factors affecting  
543 anthocyanin accumulation in plant tissues [29, 35]. Generally, low temperature increases  
544 anthocyanin concentration, whereas elevated temperature decreases it. Of the *Cymbidium*  
545 floral organs, the tepals showed significantly lower anthocyanin concentrations under  
546 high temperatures (Fig. 6C). However, no significant reduction in the concentration of  
547 anthocyanins in the labellum and column organs at high temperature was observed (Fig.  
548 6C). Thus, anthocyanin accumulation in the tepal organ showed a different response at  
549 high temperature than that in the labellum organs, which was the other petal-like floral  
550 organ. On the other hand, no marked changes in flavonol concentrations were observed

551 in any of the floral organs (Fig. 6D). This result suggested that the accumulation of  
552 flavonols had been completed by stage 2, at which the plant material was moved to the  
553 high growth temperature, since flavonols are synthesized during the early floral  
554 developmental stage (Fig. 1D). In rose (*Rosa hybrida*), the expression levels of *CHS* and  
555 *DFR* decreased by 50% after heat treatment (39°C/18°C), suggesting that the decreased  
556 anthocyanin concentration was due, at least in part, to reduced transcription of these genes  
557 [29, 35]. In the Oriental hybrid lily “Marrero,” elevated temperature caused low  
558 coloration in the tepal organs at stages 2 and 3, during which increasing concentrations  
559 of anthocyanins would usually accumulate [30]. It has also been reported that anthocyanin  
560 accumulation in petunia petals was increased by low-temperature incubation [25, 26]. The  
561 expression levels in lily of the *LhMYB12*, *CHS*, *F3H*, and *DFR* genes was suppressed  
562 under a high-temperature treatment (30°C/25°C) compared with a low-temperature  
563 treatment (20°C/15°C) [30]. Therefore, the reduced transcription of *LhMYB12*, which is  
564 a key anthocyanin biosynthesis regulatory gene, caused by high temperature, was  
565 responsible for the reduced anthocyanin accumulation in lily tepals under these conditions  
566 [30]. In the present study, when *Cymbidium Sazanami* ‘Champion’ was exposed to high  
567 temperatures, a marked decrease in the expressions of *CyMYB1*, *CyDFR*, and *CyANS* was  
568 detected in the tepal organs (Fig. 7). The expressions of these three genes in the labellum  
569 were also suppressed under high temperatures, but they were higher than those in the  
570 tepals. Therefore, tepal organ-specific anthocyanin suppression was thought to result  
571 from the suppression of *CyMYB1* at high temperatures. In addition, this finding strongly  
572 suggests that *CyMYB1* is directly regulate the transcription of the two late anthocyanin  
573 biosynthesis genes, *CyDFR* and *CyANS*, in *Cymbidium* floral organs.

574 Thus, we demonstrated that organ-specific and temperature-dependent anthocyanin  
575 pigmentation could be regulated by a *CyMYB1* in *Cymbidium* hybrid flowers, and the



576 CyMYB1 interacts with CybHLH1/2, with this complex activating the transcription of  
577 *CyDFR* and *CyANS*. Moreover, we demonstrated that the reduced anthocyanin  
578 concentration in the tepals developing at high temperatures was associated with reduced  
579 expression of *CyMYB1*.

580

#### 581 **Declaration of interest**

582 None.

583

#### 584 **Author's contribution**

585 T. Nakatsuka, T. Suzuki, H. Dohra, and H. Ohno conceived and designed the  
586 experiments. T. Nakatsuka, T. Suzuki, H. Dohra, K. Harada and Y. Kobayashi carried out  
587 the experiments. T. Nakatsuka wrote the paper. T. Suzuki, H. Dohra and H. Ohno edited  
588 the manuscripts. All authors reviewed the results and approved the final version of the  
589 manuscript.

590

#### 591 **Finding**

592 This study was supported by KAKENHI Grant Number 26450032, Japan Society  
593 for Promotion of Science, and by the Program to Disseminate Tenure Tracking System,  
594 Japan Science and Technology Agency.

595

#### 596 **Acknowledgements**

597 We thank Dr. Fumi Tatsuzawa, Iwate University, to help flavonoid analysis.

598

#### 599 **References**

600 [1] F. Tatsuzawa, N. Saito, M. Yokoi, Anthocyanins in the flowers of *Cymbidium*,

- 601 Lindleyana, 11 (1996) 214-219.
- 602 [2] J. Arditti, Fundamentals of Orchid Biology, John Wiley and Sons, New York, 1992.
- 603 [3] K.M. Davies, Modifying anthocyanin production in flowers, in: K. Gould, K. Davies,  
604 C. Winefield (Eds.) Anthocyanins Biosynthesis, Functions, and Applications,  
605 Springer, New York, 2009, pp. 49-83.
- 606 [4] J. Mol, E. Grotewold, R. Koes, How genes paint flowers and seeds, Trend Plant Sci,  
607 3 (1998) 212-217.
- 608 [5] C.Y. Chiou, K.W. Yeh, Differential expression of *MYB* gene (*OgMYB1*) determines  
609 color patterning in floral tissue of *Oncidium* Gower Ramsey, Plant Mol Biol, 66  
610 (2008) 379-388.
- 611 [6] C.Y. Chiou, K.W. Yeh, Coloration and color patterning in floral tissues of *Oncidium*  
612 Grwer Ramsey, in: W.H. Chen, H.H. Chen (Eds.) Orchid Biotechnology II, World  
613 Scientific, Singapore, 2011, pp. 101-115.
- 614 [7] A.D. Hieber, R.G. Mudalige-Jayawickrama, A.R. Kuehnle, Color genes in the orchid  
615 *Oncidium* Gower Ramsey: identification, expression, and potential genetic  
616 instability in an interspecific cross, Planta, 223 (2006) 521-531.
- 617 [8] C.C. Hsu, Y.Y. Chen, W.C. Tsai, W.H. Chen, H.H. Chen, Three R2R3-MYB  
618 transcription factors regulate distinct floral pigmentation patterning in *Phalaenopsis*  
619 spp, Plant Physiol, 168 (2015) 175-191.
- 620 [9] E.T. Johnson, H. Yi, B. Shin, B.J. Oh, H. Cheong, G. Choi, *Cymbidium hybrida*  
621 dihydroflavonol 4-reductase does not efficiently reduce dihydrokaempferol to  
622 produce orange pelargonidin-type anthocyanins, Plant J, 19 (1999) 81-85.
- 623 [10] L. Wang, N.W. Albert, H. Zhang, S. Arathoon, M.R. Boase, H. Ngo, K.E. Schwinn,  
624 K.M. Davies, D.H. Lewis, Temporal and spatial regulation of anthocyanin  
625 biosynthesis provide diverse flower colour intensities and patterning in *Cymbidium*

626 orchid, *Planta*, 240 (2014) 983-1002.

627 [11] T. Nakatsuka, N. Sasaki, M. Nishihara, Transcriptional regulators of flavonoid  
628 biosynthesis and their application to flower color modification in Japanese gentians,  
629 *Plant Biotechnol*, 31 (2014) 389-399.

630 [12] W. Xu, C. Dubos, L. Lepiniec, Transcriptional control of flavonoid biosynthesis by  
631 MYB-bHLH-WDR complexes, *Trends Plant Sci*, 20 (2015) 176-185.

632 [13] C. Li, J. Qiu, L. Ding, M. Huang, S. Huang, G. Yang, J. Yin, Anthocyanin  
633 biosynthesis regulation of *DhMYB2* and *DhbHLH1* in *Dendrobium* hybrid petals,  
634 *Plant Physiol Biochem*, 112 (2017) 335-345.

635 [14] N.W. Albert, S. Arathoon, V.E. Collette, K.E. Schwinn, P.E. Jameson, D.H. Lewis,  
636 H. Zhang, K.M. Davies, Activation of anthocyanin synthesis in *Cymbidium* orchids:  
637 variability between known regulators, *Plant Cell Tiss Organ Cult*, 100 (2010) 355-  
638 360.

639 [15] C.H. Fu, Y.W. Chen, Y.Y. Hsiao, Z.J. Pan, Z.J. Liu, Y.M. Huang, W.C. Tsai, H.H.  
640 Chen, OrchidBase: a collection of sequences of the transcriptome derived from  
641 orchids, *Plant Cell Physiol*, 52 (2011) 238-243.

642 [16] W.C. Tsai, C.H. Fu, Y.Y. Hsiao, Y.M. Huang, L.J. Chen, M. Wang, Z.J. Liu, H.H.  
643 Chen, OrchidBase 2.0: comprehensive collection of Orchidaceae floral  
644 transcriptomes, *Plant Cell Physiol*, 54 (2013) e7.

645 [17] J. Cai, X. Liu, K. Vanneste, S. Proost, W.C. Tsai, K.W. Liu, L.J. Chen, Y. He, Q. Xu,  
646 C. Bian, Z. Zheng, F. Sun, W. Liu, Y.Y. Hsiao, Z.J. Pan, C.C. Hsu, Y.P. Yang, Y.C.  
647 Hsu, Y.C. Chuang, A. Dievart, J.F. Dufayard, X. Xu, J.Y. Wang, J. Wang, X.J. Xiao,  
648 X.M. Zhao, R. Du, G.Q. Zhang, M. Wang, Y.Y. Su, G.C. Xie, G.H. Liu, L.Q. Li, L.Q.  
649 Huang, Y.B. Luo, H.H. Chen, Y. Van de Peer, Z.J. Liu, The genome sequence of the  
650 orchid *Phalaenopsis equestris*, *Nat Genet*, 47 (2015) 65-72.

- 651 [18] X. Li, F. Jin, L. Jin, A. Jackson, X. Ma, X. Shu, D. Wu, G. Jin, Characterization and  
652 comparative profiling of the small RNA transcriptomes in two phases of flowering  
653 in *Cymbidium ensifolium*, BMC Genomics, 16 (2015) 622.
- 654 [19] X. Li, J. Luo, T. Yan, L. Xiang, F. Jin, D. Qin, C. Sun, M. Xie, Deep sequencing-  
655 based analysis of the *Cymbidium ensifolium* floral transcriptome, PLoS One, 8  
656 (2013) e85480.
- 657 [20] F. Yang, G. Zhu, Digital gene expression analysis based on *de novo* transcriptome  
658 assembly reveals new genes associated with floral organ differentiation of the orchid  
659 plant *Cymbidium ensifolium*, PLoS One, 10 (2015) e0142434.
- 660 [21] X. Li, W. Xu, M.R. Chowdhury, F. Jin, Comparative proteomic analysis of labellum  
661 and inner lateral petals in *Cymbidium ensifolium* flowers, Int J Mol Sci, 15 (2014)  
662 19877-19897.
- 663 [22] K. Sasaki, N. Mitsuda, K. Nashima, K. Kishimoto, Y. Katayose, H. Kanamori, A.  
664 Ohmiya, Generation of expressed sequence tags for discovery of genes responsible  
665 for floral traits of *Chrysanthemum morifolium* by next-generation sequencing  
666 technology, BMC Genomics, 18 (2017) 683.
- 667 [23] K. Suzuki, T. Suzuki, T. Nakatsuka, H. Dohra, M. Yamagishi, K. Matsuyama, H.  
668 Matsuura, RNA-seq-based evaluation of bicolor tepal pigmentation in Asiatic hybrid  
669 lilies (*Lilium* spp.), BMC Genomics, 17 (2016) 611.
- 670 [24] D. Zhao, Y. Jiang, C. Ning, J. Meng, S. Lin, W. Ding, J. Tao, Transcriptome  
671 sequencing of a chimaera reveals coordinated expression of anthocyanin  
672 biosynthetic genes mediating yellow formation in herbaceous peony (*Paeonia*  
673 *lactiflora* Pall.), BMC Genomics, 15 (2014) 689.
- 674 [25] M. Shvarts, A. Borochoy, D. Weiss, Low temperature enhances petunia flower  
675 pigmentation and induces chalcone synthase gene expression, Physiol Plant, 99

676 (1997) 67-72.

677 [26] M. Shvarts, D. Weiss, A. Borochoy, Temperature effects on growth, pigmentation  
678 and post-harvest longevity of petunia flowers, *Sci Hort*, 69 (1997) 217-227.

679 [27] K. Nozaki, T. Takamura, S. Fukai, Effects of high temperature on flower colour and  
680 anthocyanin content in pink flower genotypes of greenhouse chrysanthemum  
681 (*Chrysanthemum morifolium* Ramat.), *J Hort Sci Biotechnol*, 81 (2006) 728-734.

682 [28] L. Shaked-Sachray, D. Weiss, M. Reuveni, A. Nissim-Levi, M. Oren-Shamir,  
683 Increased anthocyanin accumulation in aster flowers at elevated temperatures due to  
684 magnesium treatment, *Physiol Plant*, 114 (2002) 559-565.

685 [29] G. Dela, E. Or, R. Ovadia, A. Nissim-Levi, D. Weiss, M. Oren-Shamir, Changes in  
686 anthocyanin concentration and composition in 'Jaguar' rose flowers due to transient  
687 high-temperature conditions, *Plant Sci*, 2003 (2003) 333-340.

688 [30] Y.S. Lai, M. Yamagishi, T. Suzuki, Pigment accumulation and transcription of  
689 *LhMYB12* and anthocyanin biosynthesis genes during flower development in the  
690 Asiatic hybrid lily (*Lilium* spp.), *Plant Sci*, 132 (2011) 59-65.

691 [31] X.B. Xie, S. Li, R.F. Zhang, J. Zhao, Y.C. Chen, Q. Zhao, Y.X. Yao, C.X. You, X.S.  
692 Zhang, Y.J. Hao, The bHLH transcription factor *MdbHLH3* promotes anthocyanin  
693 accumulation and fruit colouration in response to low temperature in apples, *Plant*  
694 *Cell Environ*, 35 (2012) 1884-1897.

695 [32] K. Mori, N. Goto-Yamamoto, M. Kitayama, K. Hashizume, Loss of anthocyanins in  
696 red-wine grape under high temperature, *J Exp Bot*, 58 (2007) 1935-1945.

697 [33] A. Leyva, J.A. Jarillo, J. Salinas, J.M. Martinez-Zapater, Low temperature induces  
698 the accumulation of phenylalanine ammonia-lyase and chalcone synthase mRNAs  
699 of *Arabidopsis thaliana* in a light-dependent manner, *Plant Physiol*, 108 (1995) 39-  
700 46.

- 701 [34] P.J. Christie, M.R. Alfenito, V. Walbot, Impact of low-temperature stress on general  
702 phenylpropanoid and anthocyanin pathways: Enhancement of transcript abundance  
703 and anthocyanin pigmentation in maize seedlings, *Planta*, 194 (1994) 541-549.
- 704 [35] D. Weiss, Regulation of flower pigmentation and growth: Multiple signaling  
705 pathways control anthocyanin synthesis in expanding petals, *Physiol Plant*, 110  
706 (2000) 152-157.
- 707 [36] M. Martin, Cutadapt removes adapter sequences from high-throughput sequencing  
708 reads, *EMBnet J*, 17 (2011) 10-12.
- 709 [37] M.G. Grabherr, B.J. Haas, M. Yassour, J.Z. Levin, D.A. Thompson, I. Amit, X.  
710 Adiconis, L. Fan, R. Raychowdhury, Q. Zeng, Z. Chen, E. Mauceli, N. Hacohen, A.  
711 Gnirke, N. Rhind, F. di Palma, B.W. Birren, C. Nusbaum, K. Lindblad-Toh, N.  
712 Friedman, A. Regev, Full-length transcriptome assembly from RNA-seq data  
713 without a reference genome, *Nat Biotechnol*, 29 (2011) 644-652.
- 714 [38] S. Gotz, J.M. Garcia-Gomez, J. Terol, T.D. Williams, S.H. Nagaraj, M.J. Nueda, M.  
715 Robles, M. Talon, J. Dopazo, A. Conesa, High-throughput functional annotation and  
716 data mining with the Blast2GO suite, *Nucleic Acids Res*, 36 (2008) 3420-3435.
- 717 [39] J.D. Thompson, D.G. Higgins, T.J. Gibson, Improved sensitivity of profile searches  
718 through the use of sequence weights and gap excision, *Comput Appl Biosci*, 10  
719 (1994) 19-29.
- 720 [40] K. Tamura, G. Stecher, D. Peterson, A. Filipski, S. Kumar, MEGA6: Molecular  
721 Evolutionary Genetics Analysis version 6.0, *Mol Biol Evol*, 30 (2013) 2725-2729.
- 722 [41] I.M. Zimmermann, M.A. Heim, B. Weisshaar, J.F. Uhrig, Comprehensive  
723 identification of *Arabidopsis thaliana* MYB transcription factors interacting with  
724 R/B-like BHLH proteins, *Plant J*, 40 (2004) 22-34.
- 725 [42] A. Nakatsuka, M. Yamagishi, M. Nakano, K. Tasaki, N. Kobayashi, Light-induced

- 726 expression of basic helix-loop-helix genes involved in anthocyanin biosynthesis in  
727 flowers and leaves of Asiatic hybrid lily, *Sci Hort*, 121 (2009) 84-91.
- 728 [43] M. Yamagishi, How genes paint lily flowers: Regulation of colouration and  
729 pigmentation patterning, *Sci Hort*, 163 (2013) 27-36.
- 730 [44] M. Yamagishi, Y. Shimoyamada, T. Nakatsuka, K. Masuda, Two *R2R3-MYB* genes,  
731 homologs of petunia *AN2*, regulate anthocyanin biosyntheses in flower tepals, tepal  
732 spots and leaves of asiatic hybrid lily, *Plant Cell Physiol*, 51 (2010) 463-474.
- 733 [45] T. Nakatsuka, K.S. Haruta, C. Pitaksuthepong, Y. Abe, Y. Kakizaki, K. Yamamoto,  
734 N. Shimada, S. Yamamura, M. Nishihara, Identification and characterization of  
735 *R2R3-MYB* and *bHLH* transcription factors regulating anthocyanin biosynthesis in  
736 gentian flowers, *Plant Cell Physiol*, 49 (2008) 1818-1829.
- 737 [46] A.C. Allan, R.P. Hellens, W.A. Laing, MYB transcription factors that colour our fruit,  
738 *Trends Plant Sci*, 13 (2008) 99-102.
- 739 [47] N. Albert, K. Davies, K. Schwinn, Gene regulation networks generate diverse  
740 pigmentation patterns in plants, *Plant Signal Behav*, 9 (2014) 962-980.
- 741 [48] K. Petroni, C. Tonelli, Recent advances on the regulation of anthocyanin synthesis  
742 in reproductive organs, *Plant Sci*, 181 (2011) 219-229.
- 743 [49] P.K. Boss, C. Davies, S.P. Robinson, Analysis of the expression of anthocyanin  
744 pathway genes in developing *Vitis vinifera* L. Mist. Shiraz grape berries and the  
745 Implications for pathway regulation, *Plant Physiol*, 111 (1996) 1059-1066.
- 746 [50] M.C. Cutanda-Perez, A. Ageorges, C. Gomez, S. Vialet, N. Terrier, C. Romieu, L.  
747 Torregrosa, Ectopic expression of *VlmybA1* in grapevine activates a narrow set of  
748 genes involved in anthocyanin synthesis and transport, *Plant Mol Biol*, 69 (2009)  
749 633-648.
- 750 [51] A.R. Rinaldo, E. Cavallini, Y. Jia, S.M. Moss, D.A. McDavid, L.C. Hooper, S.P.

751 Robinson, G.B. Tornielli, S. Zenoni, C.M. Ford, P.K. Boss, A.R. Walker, A grapevine  
752 anthocyanin acyltransferase, transcriptionally regulated by *VvMYBA*, can produce  
753 most acylated anthocyanins present in grape skins, *Plant Physiol*, 169 (2015) 1897-  
754 1916.

755

## 756 **Figure legends**

757 **Figure 1. Temporal and spatial accumulation patterns of flavonoids in *Cymbidium***  
758 **‘Mystique’ floral organs.**

759 **A.** The different organs of the orchid flowers are given in white letters as follows: S, petal-  
760 like sepal; P, lateral petal; L, labellum; C, column. Tepal is a general term for both petal-  
761 like sepals and lateral petals. Bar = 1 cm.

762 **B.** Flower developmental stages (Stages (S) 1 to 4) as described in the Materials and  
763 methods section. Bar = 1 cm.

764 **C.** Anthocyanin accumulation profiles of different floral organs of *Cymbidium* ‘Mystique’  
765 during flower development. Value and error bars indicate the mean  $\pm$  standard error (n =  
766 5). Cy3G, cyanidin 3-*O*-glucoside; Cy3R, cyanidin 3-*O*-rutinoside; Pe3R, peonidin 3-*O*-  
767 rutinoside; Cy3MG, cyanidin 3-malonylglucoside.

768 **D.** Flavonol accumulation profiles of different floral organs of *Cymbidium* ‘Mystique’  
769 during flower development. The flavonol concentration was determined from the peak  
770 area detected at 360 nm. Value and error bars indicate the mean  $\pm$  standard error (n = 5).

771

772 **Figure 2. Phylogenetic tree inferred from the amino acid sequences of the R2R3**  
773 **region of CyMYBs with R2R3-MYB from other species.**

774 This phylogenetic tree was constructed by the neighbor-joining method with 1,000  
775 bootstrapping data sets. R2R3-MYB name and GenBank accession number are indicated



776 as follows: *Antirrhinum majus* MIXTA (Q38739), MYB305(P81391), PHAN (O65366),  
777 ROSEA1 (ABB83826), ROSEA2 (ABB8327), and VENOSA (ABB83828); *Arabidopsis*  
778 *thaliana* AS1 (O80931), ATR1 (O64399), GL1 (P27900), MYB2 (Q39028), MYB12  
779 (O22264), PAP1 (Q9FE25), PAP2 (Q9ZTC3), PCMYB1 (Q9S7G7), TT2 (Q9FJA2), and  
780 WER (Q9SEI0); *Cymbidium* hybrid CyMYB1 to CyMYB16 (in this study); *Dendrobium*  
781 hybrid MYB1 (K7ZBK1) and MYB2 (A0A1S6JNE7); *Gentiana triflora* MYB3  
782 (A9ZMI4), MYBP3 (L0N1P2), and MYBP4 (A9ZMI5); *Hordeum vulgare* GAMYB  
783 (Q96464); *Lilium* hybrid MYB6 (D4QF65) and MYB12 (D4QF64); *Nicotiana tabacum*  
784 MYBA1 (Q948S6); *Oncidium* hybrid MYB1 (A7KTI5); *Phalaenopsis* ssp. MYB2  
785 (A0A096ZX46), MYB11 (A0A096ZX39), and MYB12 (A0A096ZX55); *Petunia*  
786 *hybrida* AN2 (Q9M72) and MYBPH3 (Q02992); *Vitis vinifera* MYBA1-1 (Q8L5P3); *Zea*  
787 *mays* C1 (P10290), P (P27898), Pl (O22450) and RS2 (Q9S7B2). Scale bar represents 0.1  
788 substitution per site.

789

### 790 **Figure 3. Protein–protein interaction between CyMYB1 and CybHLHs**

791 The CyMYB1, CybHLH1, and CybHLH2 proteins were fused to the GAL4 DNA-binding  
792 domain or to the GAL4 activation domain. pGBKT7 and pGADT7 are the negative  
793 controls for bait and prey, respectively. Yeast was grown on double-selection medium  
794 (–Leu, –Trp) and quadruple-selection medium (–Leu, –Trp, –His, –Ade) supplemented  
795 with 15 mM 3-AT at 30°C for 2 to 3 days.

796

### 797 **Figure 4. Relative expression levels of anthocyanin biosynthesis regulatory genes in** 798 **each floral organ of *Cymbidium* hybrid ‘Mystique’ during flower development**

799 Value and error bars are the mean  $\pm$  standard error (n = 6).

800

801 **Figure 5. Relative expression levels of anthocyanin and flavonol biosynthesis**  
802 **structural genes in each floral organ of *Cymbidium* hybrid ‘Mystique’ during flower**  
803 **development**

804 Value and error bars are the mean  $\pm$  standard error (n = 6).

805

806 **Figure 6. Effect of growth temperature on flower pigmentation of *Cymbidium***  
807 **Sazanami ‘Champion’**

808 **A)** *Cymbidium* flowers grown at 20°C/15°C (L). **B)** *Cymbidium* flowers grown at  
809 30°C/25°C (H). Bar = 1 cm.

810 **C)** Anthocyanin concentration profiles of each floral organ of *Cymbidium* Sazanami  
811 ‘Champion’ grown at different temperatures. Value and error bars indicate the mean  $\pm$   
812 standard error (n = 5). Cy3G, cyanidin 3-*O*-glucoside; Cy3R, cyanidin 3-*O*-rutinoside;  
813 Pe3R, peonidin 3-*O*-rutinoside; Cy3MG, cyanidin 3-malonylglucoside.

814 **D)** Flavonol concentration profiles of each floral organ of *Cymbidium* Sazanami  
815 ‘Champion’ grown at different temperatures. Flavonol concentrations were determined  
816 from the peak area detected at 360 nm. Asterisks indicate statistically significant  
817 difference between the 20°C/15°C (L) and 30°C/25°C (H) treatments using the Student’s  
818 *t*-test (\*\*,  $P < 0.01$ ).

819

820 **Figure 7. Effect of growth temperature on the expression levels of anthocyanin**  
821 **biosynthesis-related genes of *Cymbidium* Sazanami ‘Champion’**

822 Relative expression levels of *Cymbidium* anthocyanin biosynthesis regulatory and  
823 enzymatic genes in each floral organ of *Cymbidium* Sazanami ‘Champion’ grown at  
824 different temperatures. S2 is a sample at stage 2 before temperature treatment. L and H  
825 are samples collected at stage 4 after they were grown at 20°C/15°C and 30°C/25°C,

826 respectively. Value and error bars are the mean  $\pm$  standard error (n = 6).

827

828 **Supplementary Figure S1. Regulation of the anthocyanin biosynthesis pathway by**  
829 **the transcription factor CyMYB1**

830 CHS, chalcone synthase; CHI, chalcone isomerase; F3H, flavanone 3-hydroxylase;  
831 F3'H, flavonoid 3'-hydroxylase; DFR, dihydroflavonol 4-reductase; ANS, anthocyanidin  
832 synthase; 3GT, anthocyanidin 3-O-glucosyltransferase; 3RT, UDP-rhamnose:  
833 anthocyanin 3-O-glucoside-rhamnosyltransferase; MalT, anthocyanin: malonyl-CoA  
834 acyltransferase; FLS, flavonol synthase. Blue characterized genes were identified in  
835 current study. This study indicated that *CyMYB1* was key regulatory gene for tepal- and  
836 temperature-dependent anthocyanin accumulation to activate transcription of *CyDFR* and  
837 *CyANS* in *Cymbidium*.

838

839 **Supplementary Figure S2. Phylogenetic tree inferred from amino acid sequences of**  
840 ***bHLH* genes from *Cymbidium* and other species**

841 This phylogenetic tree was constructed by the neighbor-joining method with 1,000  
842 bootstrapping data sets. bHLH name and GenBank accession number are indicated as  
843 follows: *Antirrhinum majus* delila (Q38736), *Arabidopsis thaliana* MYC1 (Q8W2F1),  
844 EGL1 (Q9CAD0), GL3 (Q9FN69), and TT8 (Q9FT81), *Cymbidium* hybrid bHLH1 and  
845 bHLH2 (in this study), *Dendrobium* hybrid (A0A1S6JNE8), *Gentiana triflora* (B7XE11|),  
846 *Gerbera hybrida* (O82686), *Ipomoea nil* bHLH1 (Q1JV08), bHLH2 (Q1JV07), and  
847 bHLH3 (Q1JV06), *Lilium* hybrid (Q401N5), *Oryza sativa* Ra (Q40643) and Rc (Q2I7J3),  
848 *Perilla frutescens* F3G1(Q852P3) and MYC-RP (Q9ZQS4), *Petunia hybrida* AN1  
849 (Q9FEA1), JAF13 (O64908), *Phalaenopsis* spp. (A0A096ZX60), and *Zea mays* In1  
850 (Q41875) and Lc (P13526). Scale bar represents 0.1 substitution per site.

851

852 **Supplementary Figure S3. Phylogenetic tree inferred from the amino acid sequences**  
853 **of CHI from *Cymbidium* and other species**

854 This phylogenetic tree was constructed by the neighbor-joining method with 1,000  
855 bootstrapping data sets. CHI name and GenBank accession number are indicated as  
856 follows: *Allium cepa* (Q6QHK0), *Arabidopsis thaliana* (P41088), *Camellia sinensis*  
857 (Q45QI7), *Chrysanthemum morifolium* CHI1 (A1E260) and CHI2 (A1E261), *Citrus*  
858 *sinensis* (Q9ZWR1), *Cymbidium* hybrid CHI1 and CHI2 (in this study), *Dendrobium*  
859 hybrid (V9PCX1), *Dianthus caryophyllus* (Q43754), *Elaeagnus umbellata* (O65333),  
860 *Eustoma exaltatum* (Q6BEH3), *Gentiana triflora* CHI1 (Q565D8) and CHI2  
861 (unpublished data), *Glycine max* CHI1 (B2CM87), CHI2 (B2CM88) and CHI3 (A7ISP6),  
862 *Ipomoea nil* EFP (X5IGL5), *Ipomoea purpurea* (O22604), *Lotus japonicus* CHI1  
863 (I3SU15), CHI2 (Q8H0G1), and CHI3 (I3SKD9), *Medicago sativa* (U5TRY3), *Nicotiana*  
864 *tabacum* (Q33DL3), *Oncidium* hybrid (A7KTI4), *Petunia hybrida* CHIA (P11650), CHIB  
865 (P11651), CHIC (Q9M5B3), and EFP (D7US50), *Phalaenopsis equestris*  
866 (A0A096ZX25), *Phaseolus vulgaris* (P14298), *Raphanus sativus* (O22651), *Torenia*  
867 *hybrida* CHI4B (D7US52) and EFP (D7US51), *Tricyrtis* spp. (W6JMJ6), *Tulipa*  
868 *fosteriana* (A0A088CB22), *Vitis vinifera* (P51117), and *Zea mays* (Q08704). Scale bar  
869 represents 0.1 substitution per site.

870

871 **Supplementary Figure S4. Phylogenetic tree inferred from the amino acid sequences**  
872 **of F3H, ANS, and FLS from *Cymbidium* and other species**

873 This phylogenetic tree was constructed by the neighbor-joining method with 1,000  
874 bootstrapping data sets.

875 F3H name and GenBank accession number are indicated as follows: *Actinidia*

876 *chinensis* (B8Y LW1), *Cymbidium* hybrid (this study), *Gentiana triflora* (Q59I70), *Lilium*  
877 hybrid (I7HDC7), *Lilium speciosum* (Q2L6K2), *Perilla frutescens* (O04112), *Persea*  
878 *americana* (Q40754), *Petunia hybrida* (Q07353), and *Tulipa fosteriana* (M9TGRO)

879 ANS name and GenBank accession number are indicated as follows: *Cymbidium*  
880 hybrid (this study, A0A088G9H7), *Iris hollandica* (A5HUP4), *Gentiana triflora*  
881 (Q59I71), *Lilium* hybrid (I7H3Z0), *Petunia hybrida* (P51092), *Pyrus communis* (P51091),  
882 *Torenia fournieri* (Q9AYT0), and *Tulipa gesneriana* (C7G0X5).

883 FLS name and GenBank accession number are indicated as follows: *Allium cepa*  
884 (Q84TM1), *Citrus unshiu* (Q9ZWQ9), *Cymbidium* hybrid (this study, and A0A088G4R1),  
885 *Dendrobium* hybrid (V9PCW6), *Eustoma exaltatum* (Q9M547), *Gentiana triflora*  
886 (F1SZA2), *Petunia hybrida* (Q07512), and *Tricyrtis* spp. (A0A0U5AET0). Scale bar  
887 represents 0.1 substitution per site.

888

889 **Supplementary Figure S5. Phylogenetic tree and alignment inferred from the amino**  
890 **acid sequences of F3'H predicted by *Cymbidium* hybrid and other species.**

891 A) This phylogenetic tree was constructed by the neighbor-joining method with 1,000  
892 bootstrapping data sets. *F3'H* name and GenBank accession number are indicated as  
893 follows: *Cymbidium* hybrid CyF3'H1 and CyF3'H2 (this study), *Epimedium sagittatum*  
894 (D5M8Q3), *Gentiana triflora* (Q59I68), *Gerbera hybrida* (Q38L00), *Lilium* hybrid  
895 F3'H1 (I7H3Y9), *Perilla frutescens* (Q93XJ2), *Petunia hybrida* Ht1 (Q9SBQ9),  
896 *Phalaenopsis* hybrid F3'5'H (Q3YAF0), *Torenia hybrida* (Q8S9C7), *Tricyrtis hirta*  
897 (B9A9Y6), *Tulipa fosteriana* (M9TH21), and *Vitis vinifera* (Q3C212). Scale bar  
898 represents 0.1 substitution per site.

899 B) Alignment of the full-length deduced amino acid sequences of CyF3'H1, CyF3'H2,  
900 and ChF3'H (KM186178) using ClustalW (Thompson et al., 1994). Red characters of

901 amino acid sequences show tree consensus domains, including proline rich region (PPxP),  
902 threonine-containing binding pocket for oxygen molecules required in catalysis  
903 (A/G)Gx(D/E)T(T/S), and the heme-binding domain (FxxGxRxCxG).

904

905 **Supplementary Figure S6. Phylogenetic tree inferred from the amino acid sequences**  
906 **of GT from *Cymbidium* hybrid and other species.**

907 This phylogenetic tree was constructed by the neighbor-joining method with 1,000  
908 bootstrapping data sets. GT name and GenBank accession number are indicated as  
909 follows: *Antirrhinum majus* chalcone 4'GT (Q33DV3); *Arabidopsis* At4g14090 (5GT,  
910 W8Q6K8), *Vigna mungo* 3GaT (Q9ZWS2), *Celosia cristata* cDOPA5GT (Q59J80),  
911 *Cleretum bellidiforme* cDOPA5GT, *Cymbidium* hybrid 3GT and 3RT (in this study),  
912 *Eustoma exaltatum* 5GT (A4F1Q3), *Gentiana triflora* 3GT (Q96493), 3'GT (Q8H0F2),  
913 and 5GT (B2NID7), *Ipomoea purpurea* 3GGT (Q53UH5), *Iris hollandica* 5GT (Q767C8),  
914 *Mirabilis jalapa* cDOPA5GT (Q59J81), *Perilla frutescens* 5GT (Q9ZR26), *Petunia*  
915 *hybrida* 3GT (Q9SBQ3), 3RT (Q43716), and 5GT (Q9SBQ2), *Rosa hybrida* 5,3-GT  
916 (Q2PGW5), *Scutellaria baicalensis* 7GT (Q9SXF2), *Solanum melongena* 5GT (Q43641),  
917 *Torenia hybrida* 5GT (Q9ZR25), *Verbena hybrida* 5GT (Q9ZR25), *Vitis vinifera* 3GT  
918 (P51094), and *Zea mays* 3GT (P16165).

919

920 **Supplementary Figure S7. Phylogenetic tree inferred from the amino acid sequences**  
921 **of MalT from *Cymbidium* hybrid and other species.**

922 The phylogenetic tree of BAHD acyltransferase proteins was constructed by the  
923 neighbor-joining method with 1,000 bootstrapping data sets. MalT name and GenBank  
924 accession number are indicated as described previously [51].

**Figure 1**

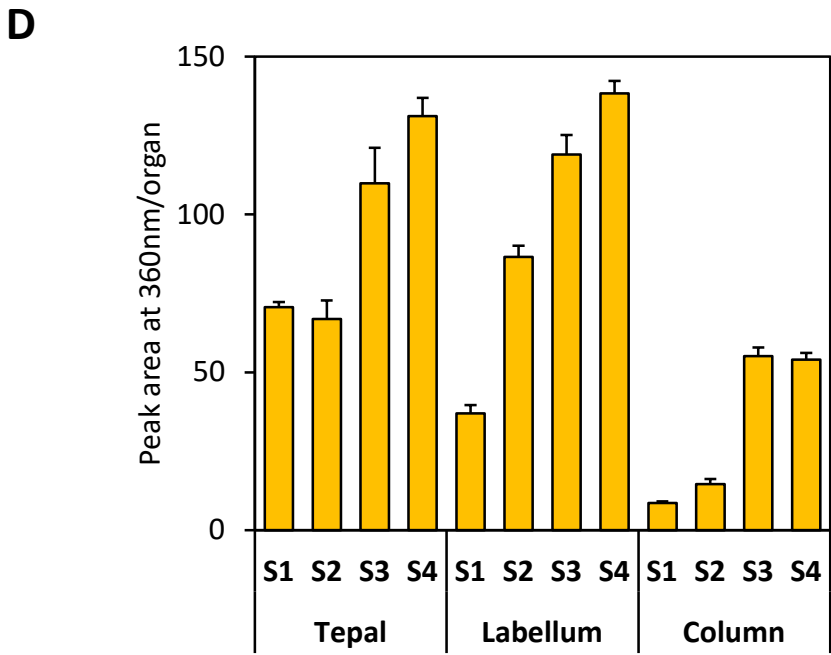
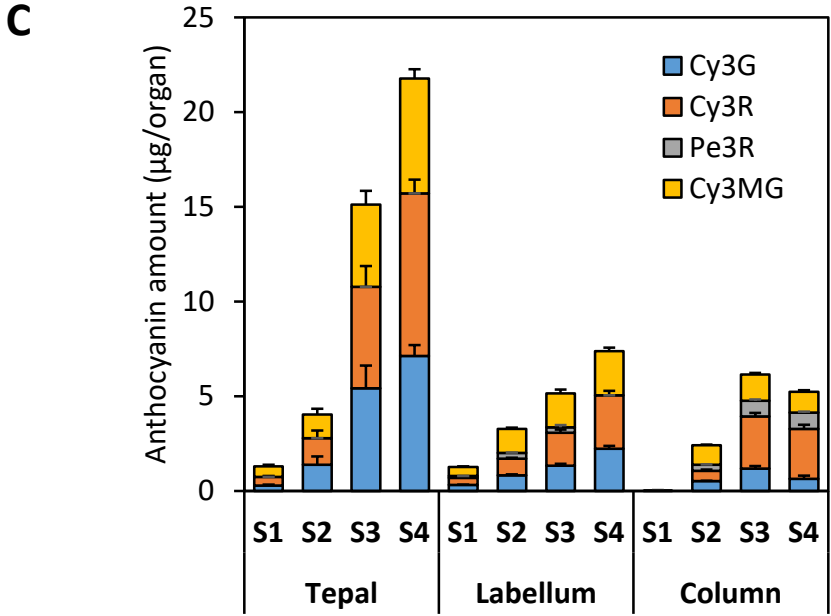


**Figure 2**

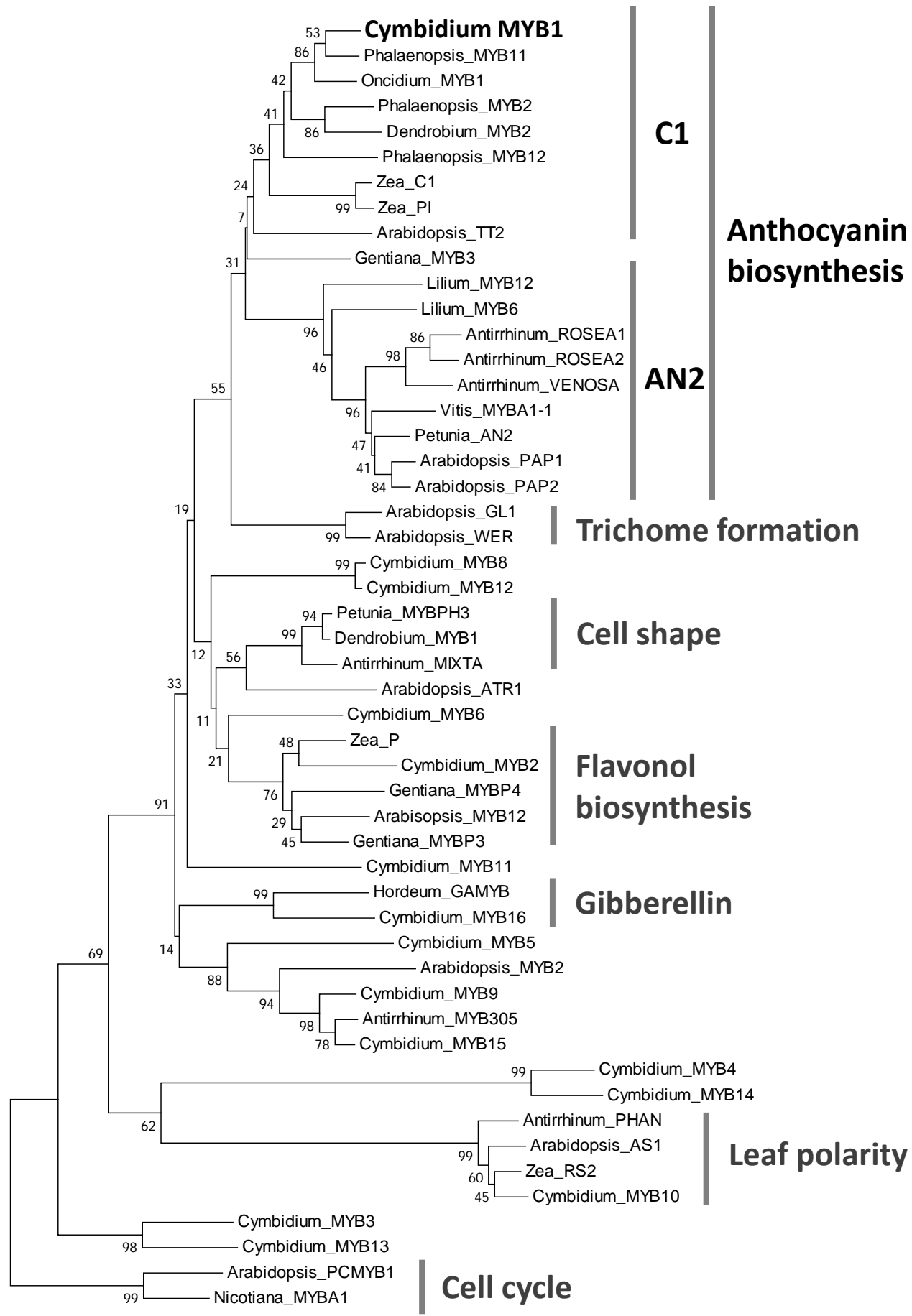




Figure 3

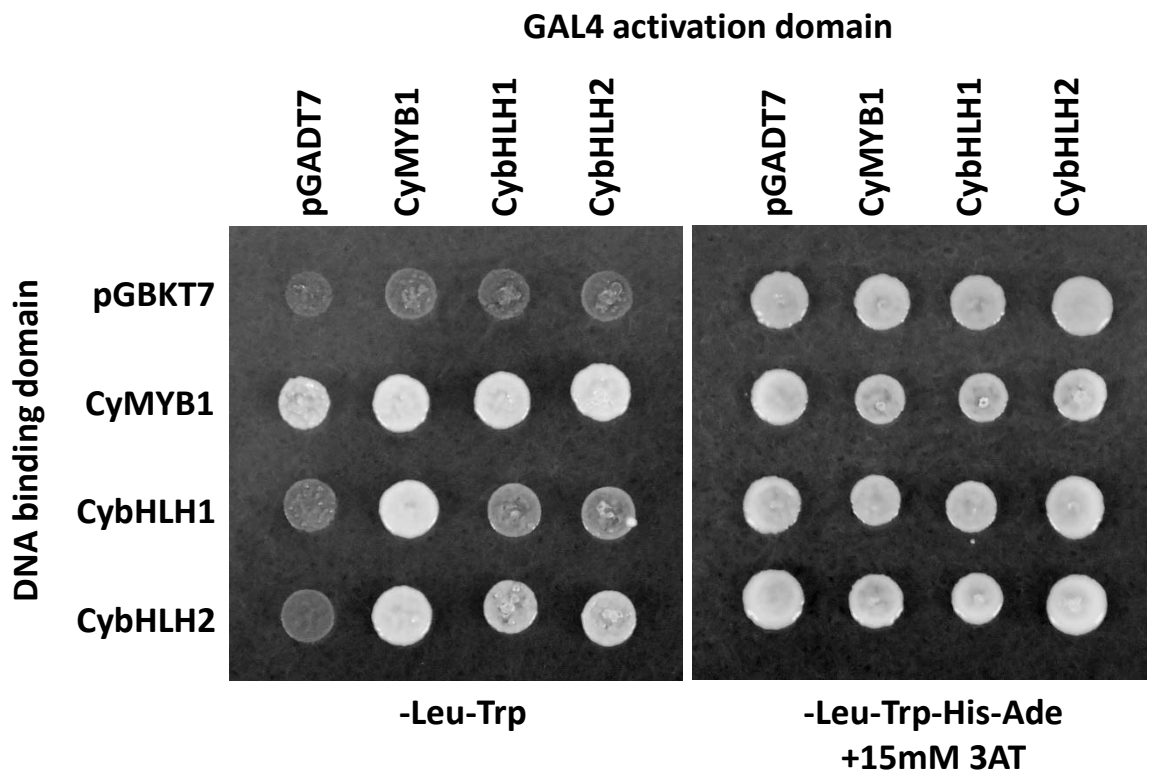
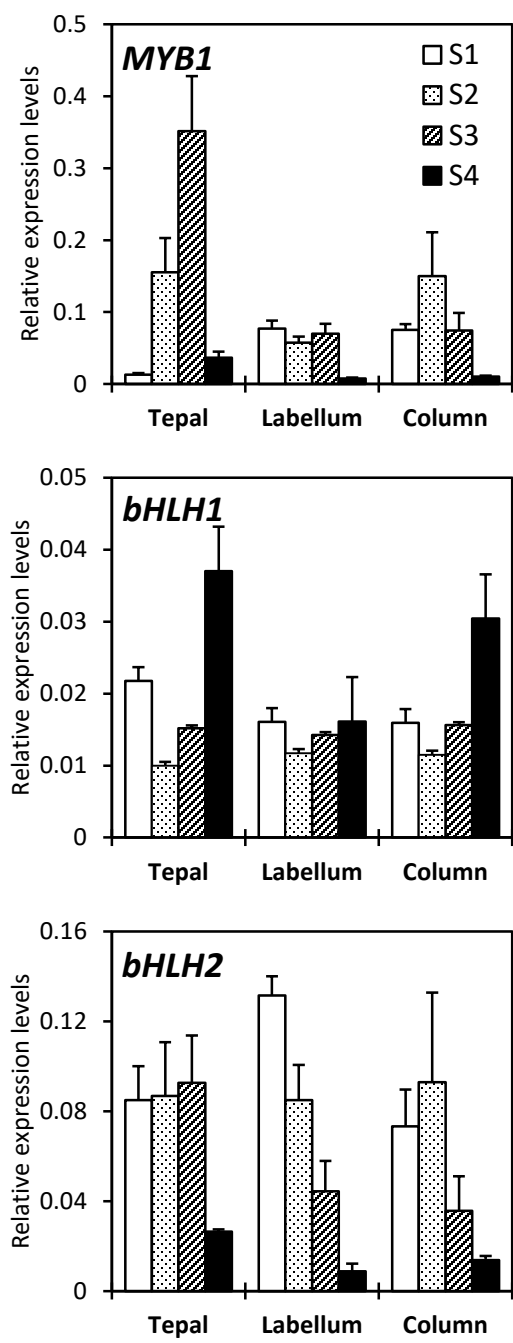


Figure 4



**Figure 5**

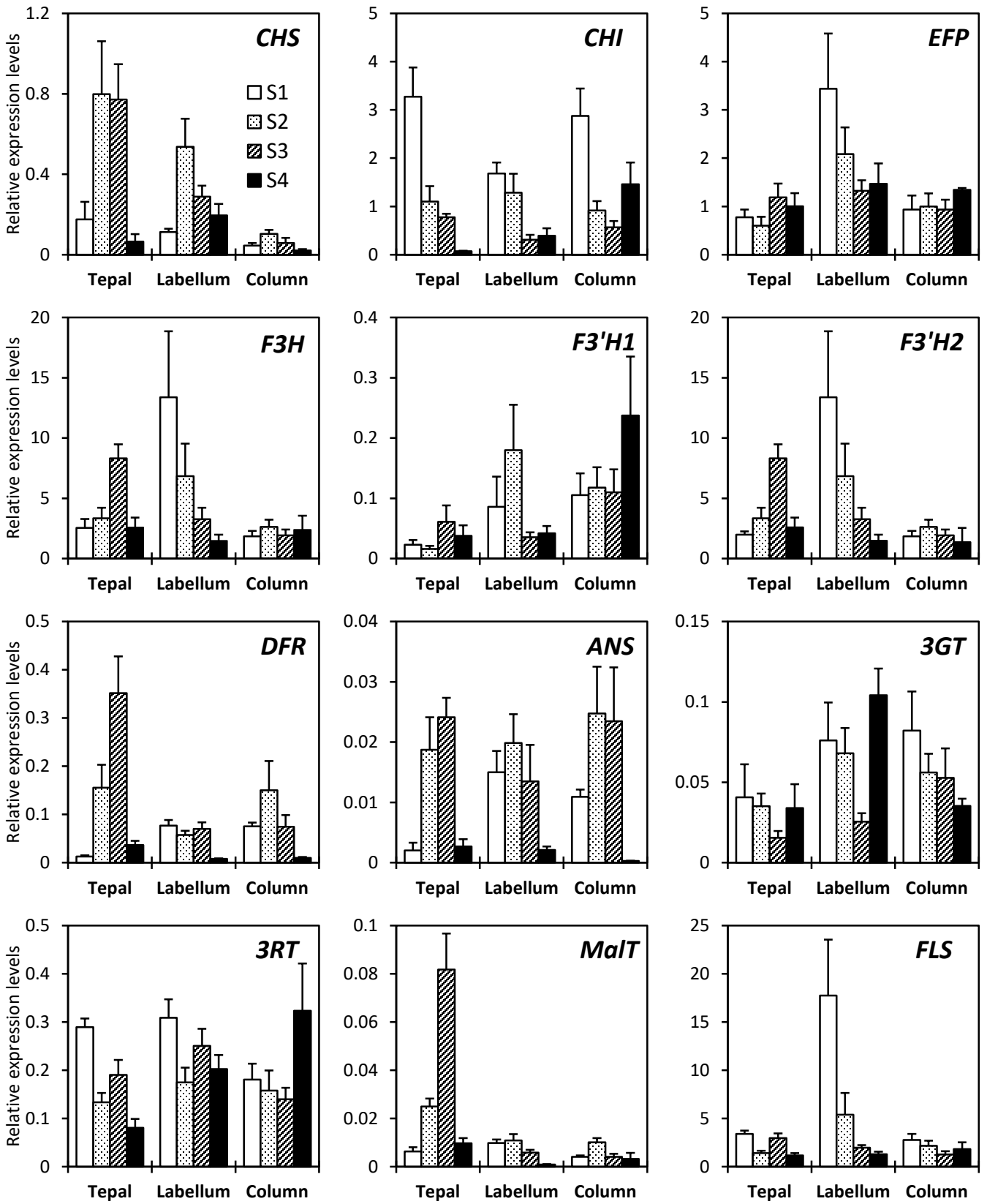
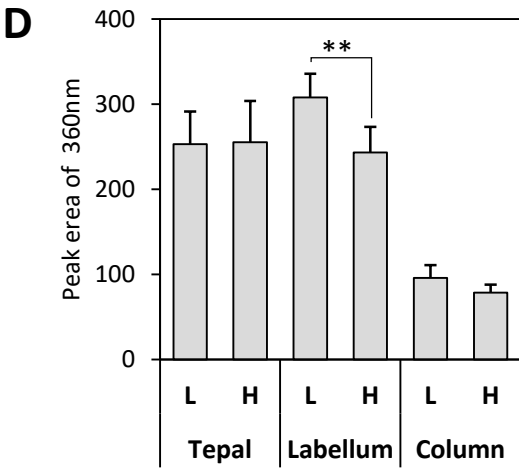
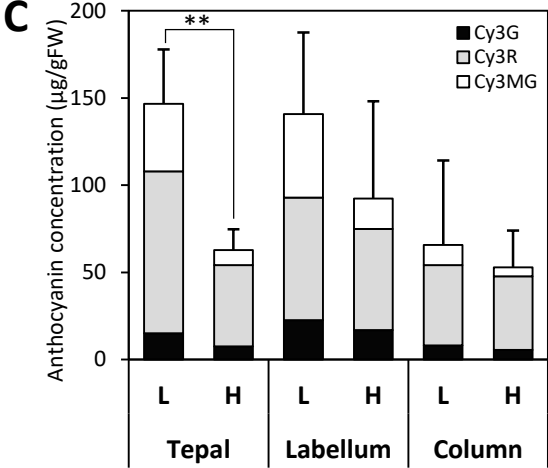
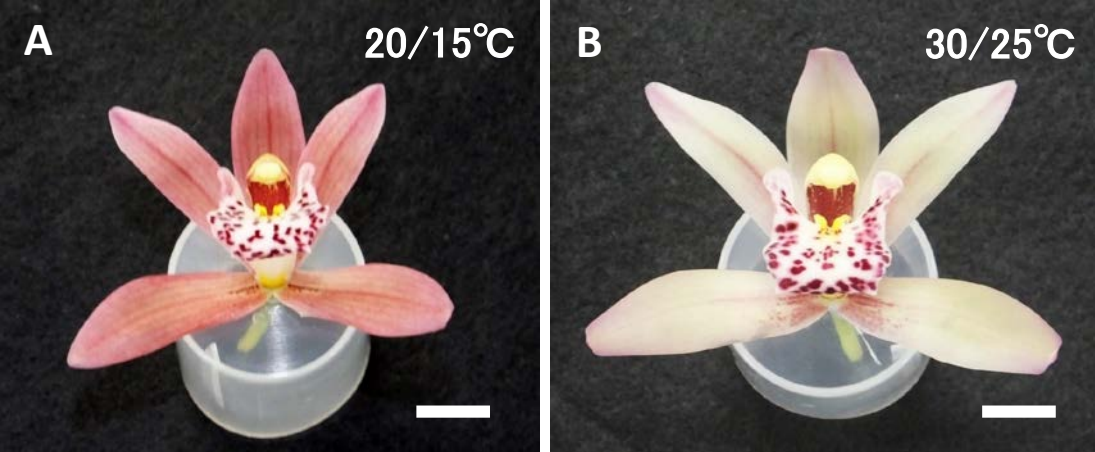
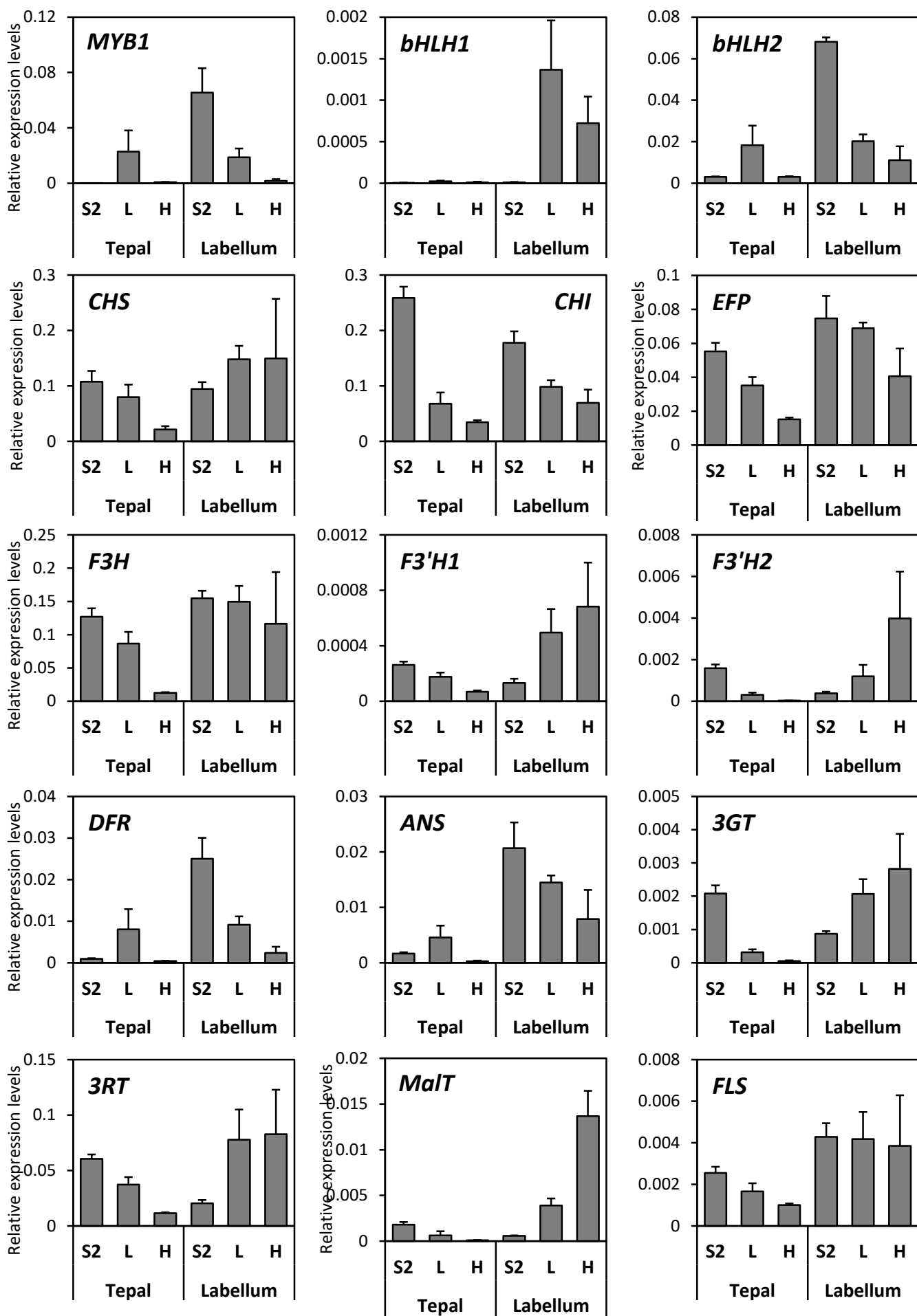


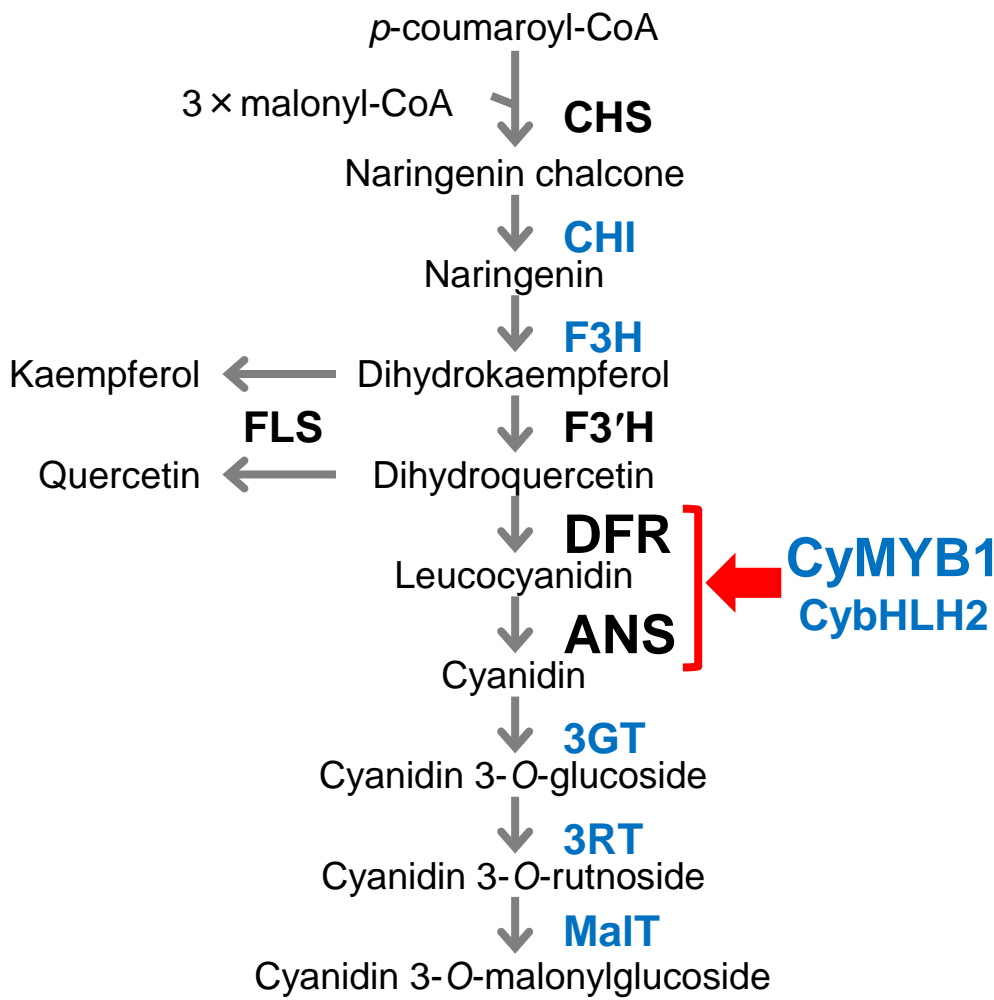
Figure 6



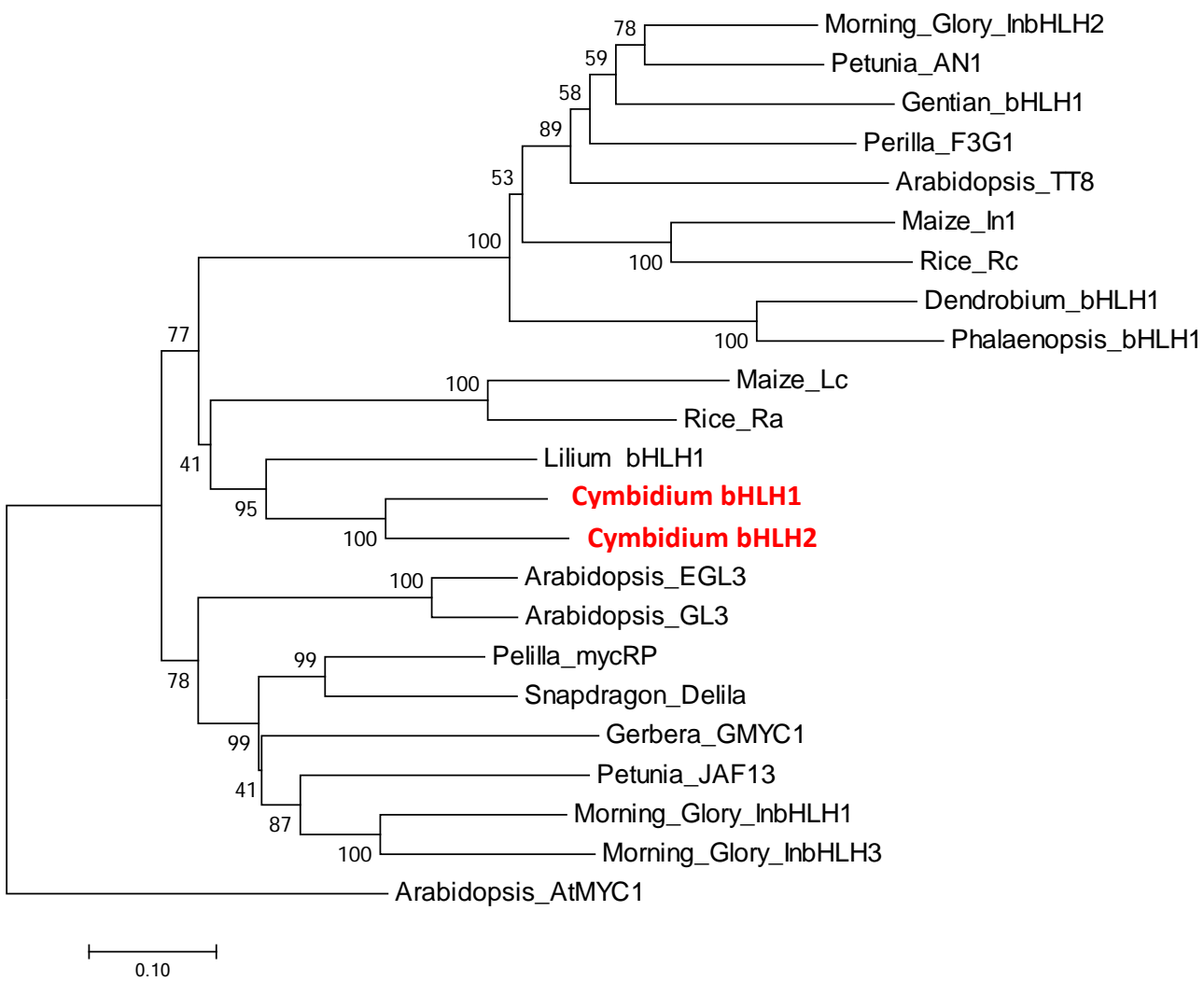
**Figure 7**



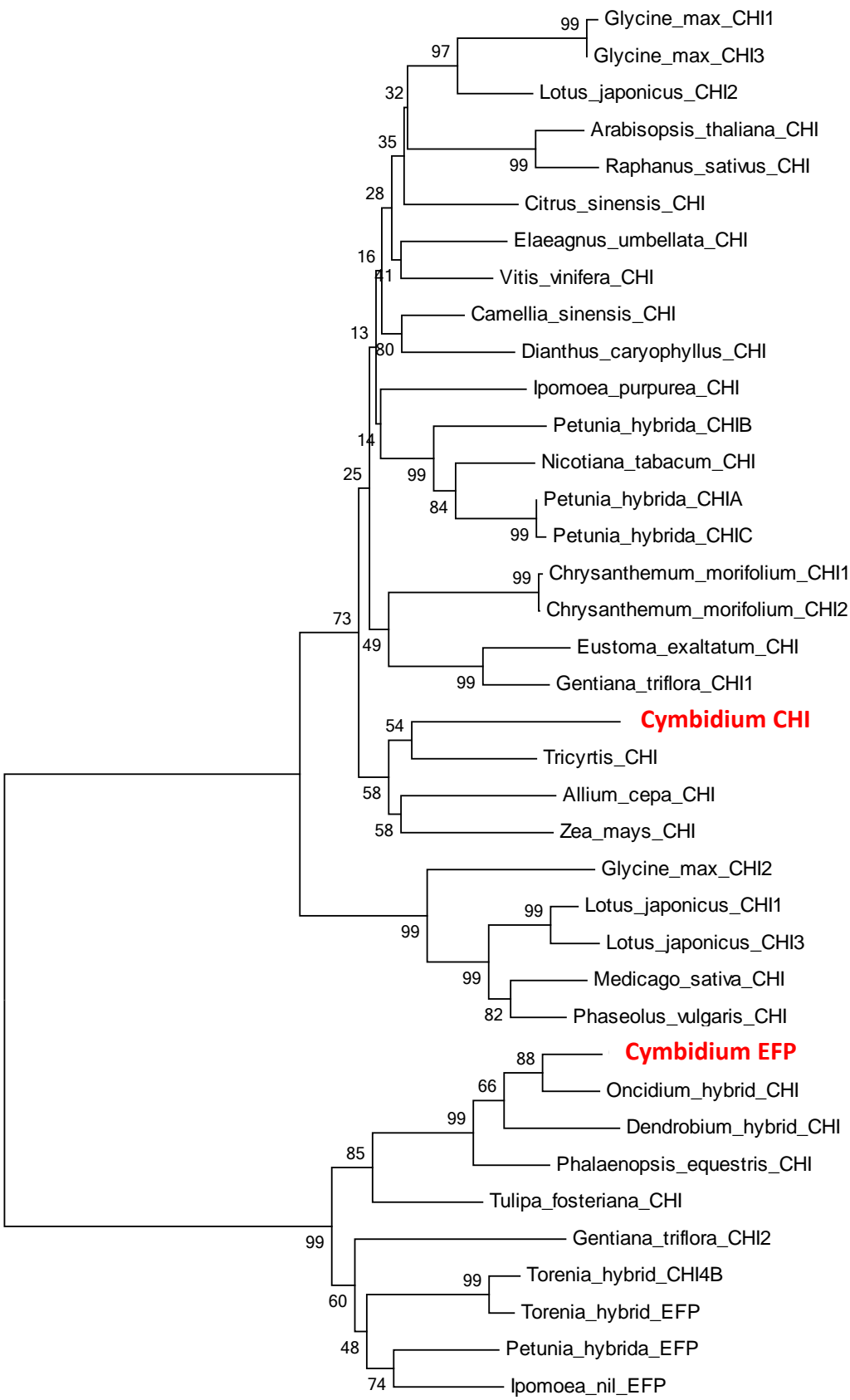
Supplementary Figure S1



Supplemental Figure S2



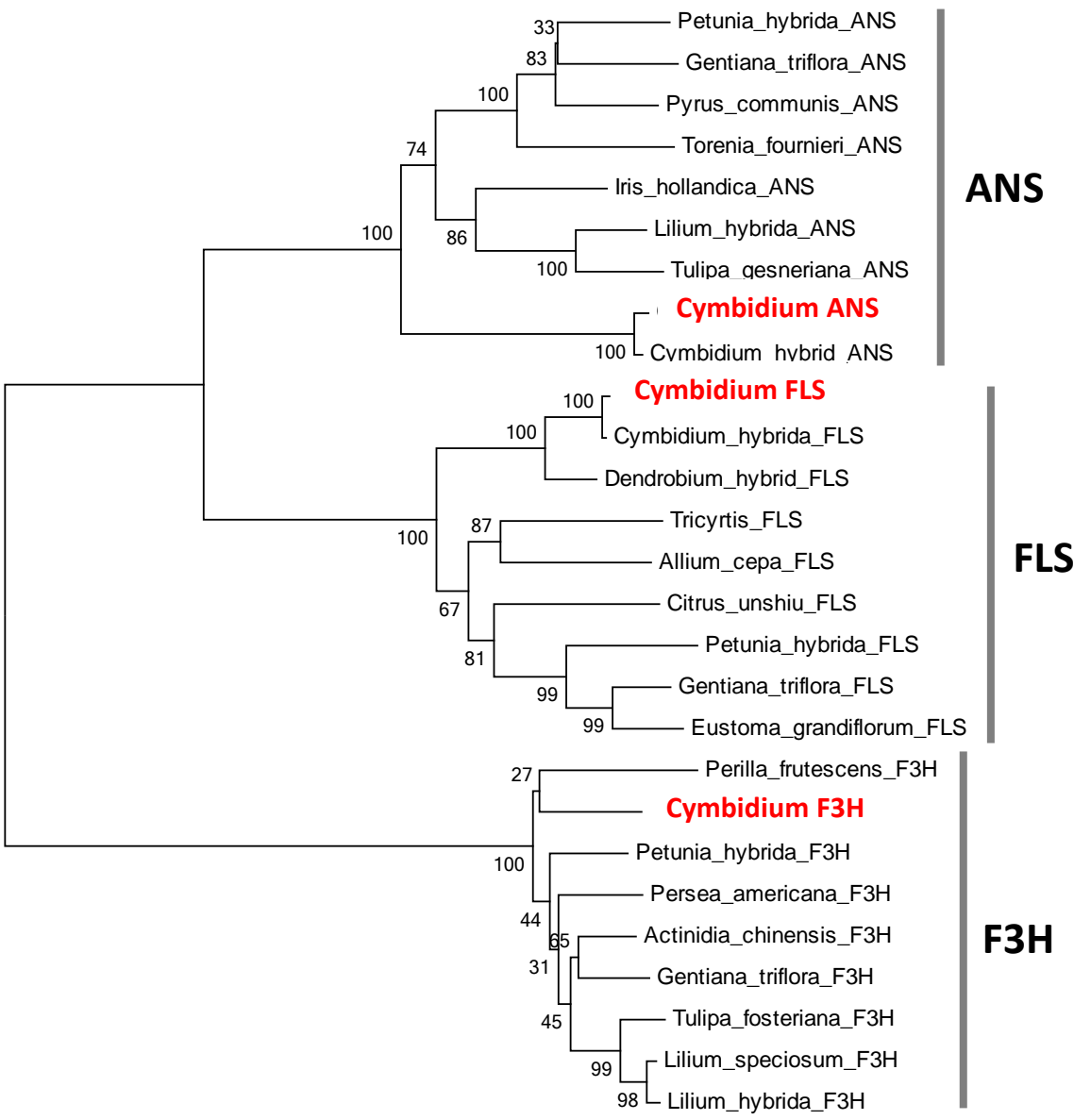
Supplemental Figure S3



0.1



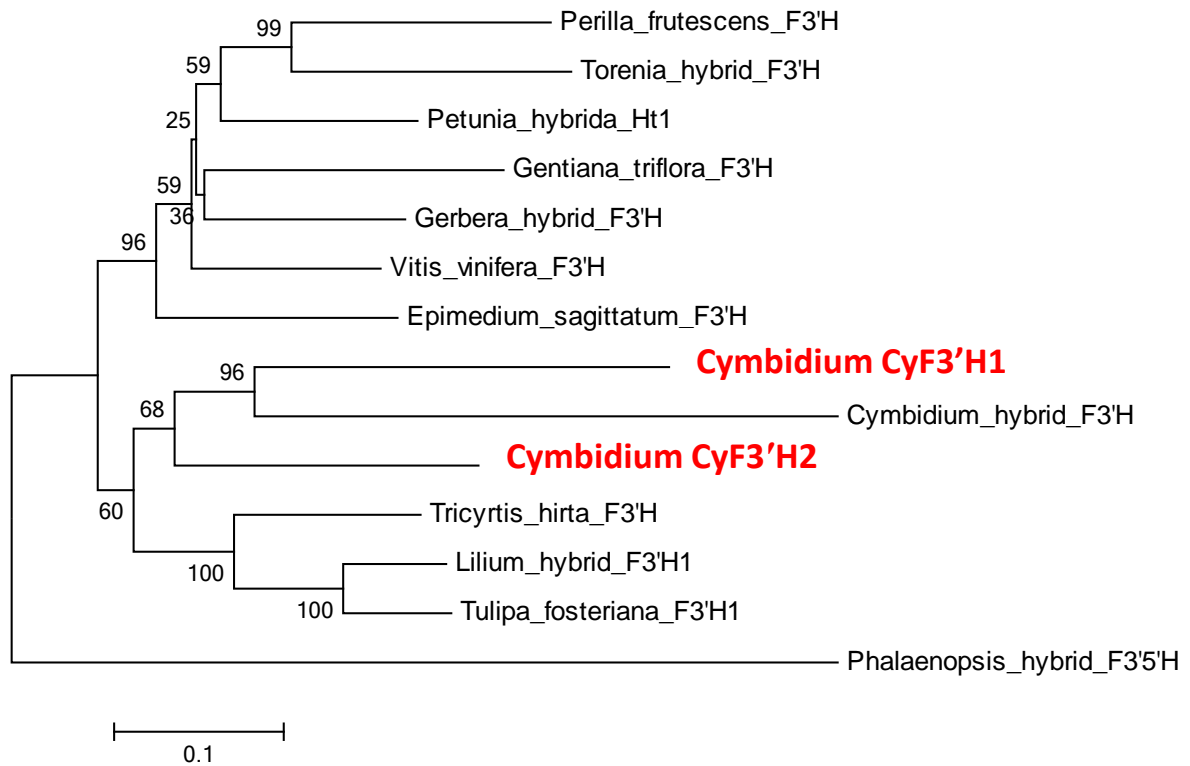
Supplemental Figure S4



0.1

# Supplemental Figure S5

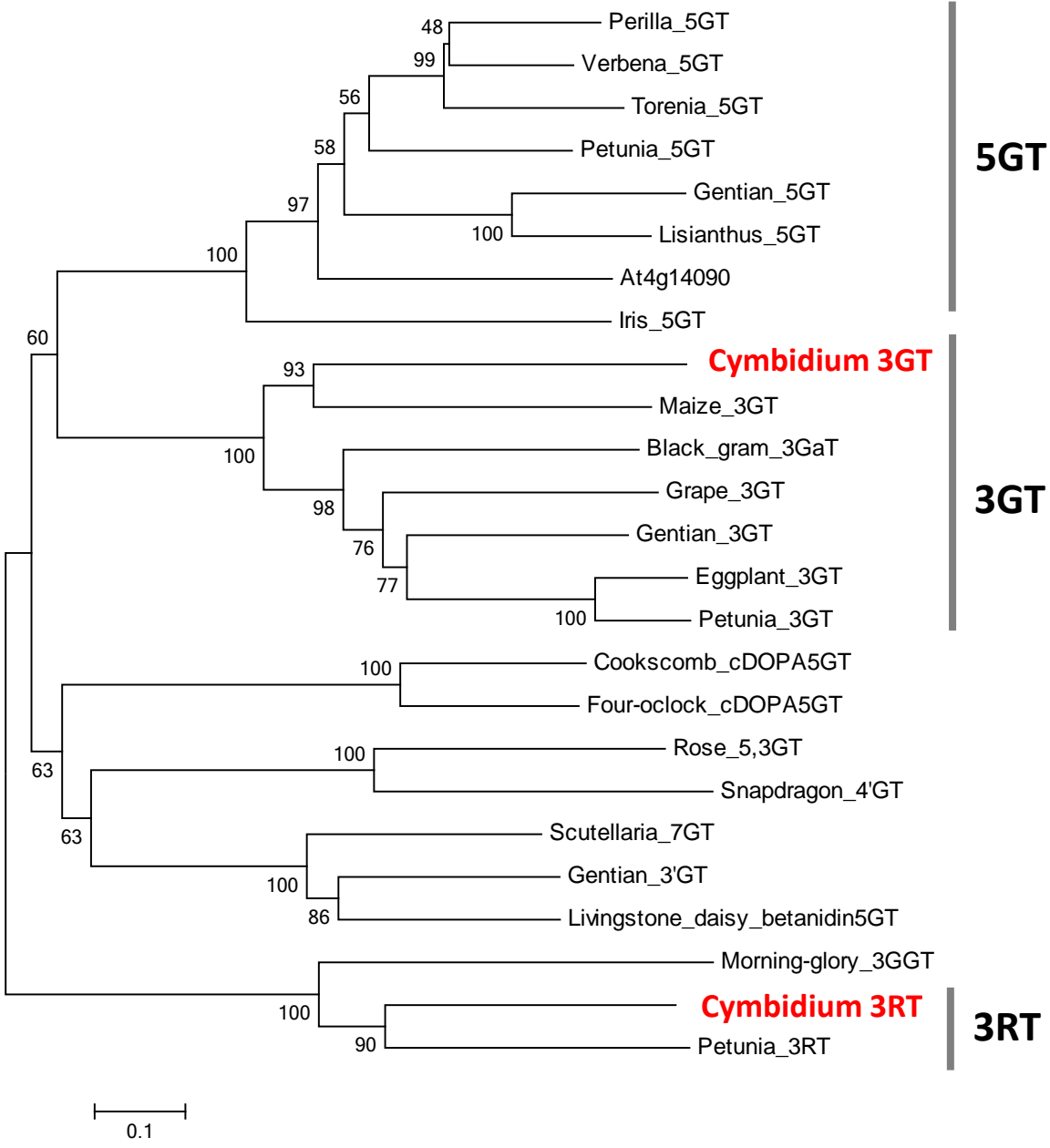
A



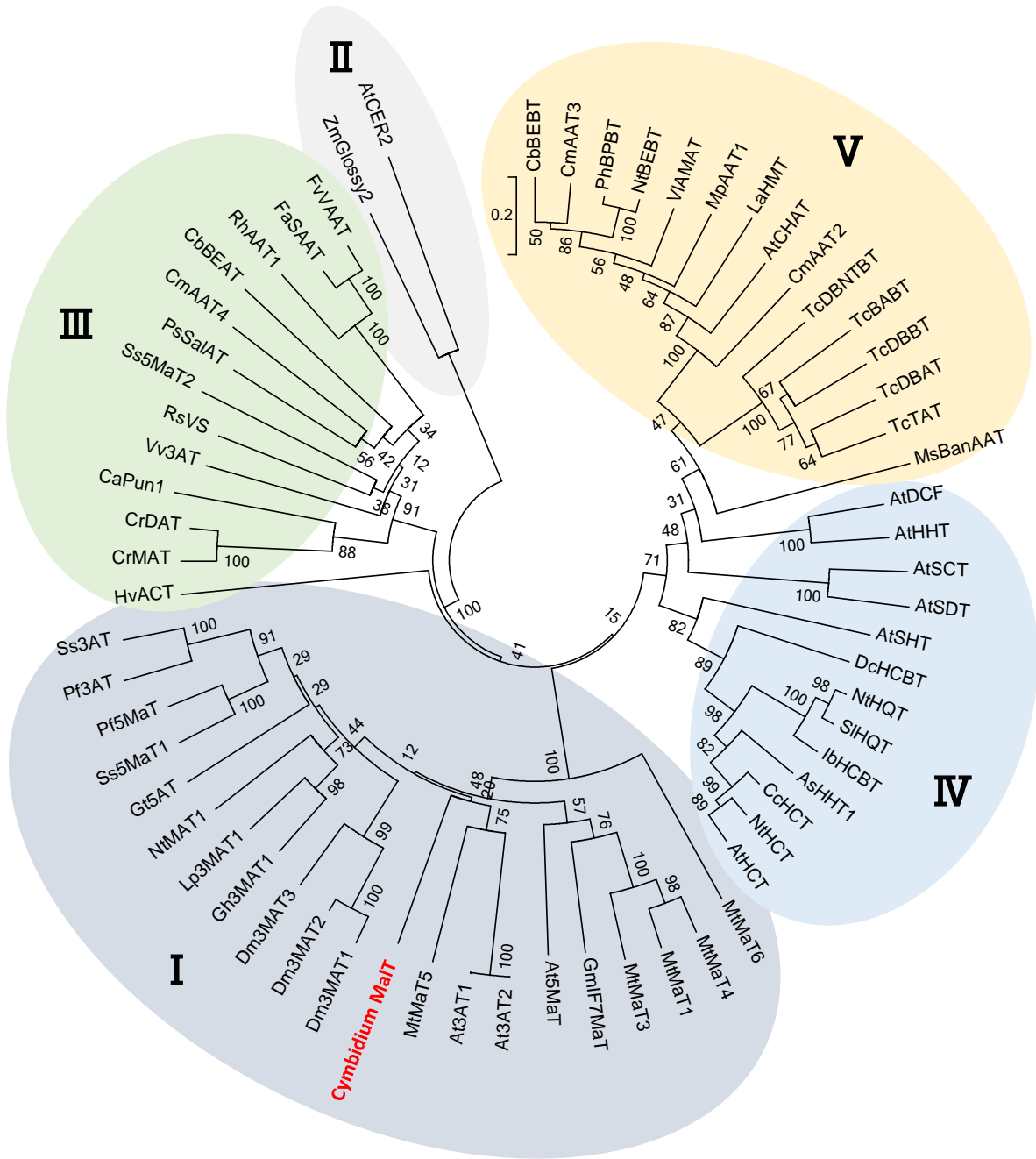
B

CyF3'H1	MAILS--LLL	VPLLLLLSAI	LLARRIRPHR	QSKLPLPPGP	KGSPILGNLL	QLGPKPHETL	YNLSKSYG--	PLIHLRFGFV
CyF3'H2	MALVI--FVL	FATILFASLL	FIVISG--DRR	RGRSNLPPGP	KGWPIIGNLP	QLGPKPHQTL	YALAKTYG--	PILRLRLGAV
ChF3'H	MAVIFTFLVF	FISVLLLLSSL	FLVGTG--R	RRRPLPPGP	KGWALLGNLL	QLGTPHRTL	QALSQSHGSA	GLLRRLRLGTV
	***: : : .	:* : * : : .	* : : *****	** . : *****	*** .*** .**	* : : : *	: : : * * *	: : * * * *
CyF3'H1	DMIVVNSAAI	AAKILR-NDA	NVASRPSSTS	VKHIAYNHQD	LIFARYGARW	RMLRKICALQ	LFSPKAMEDL	APVRADEVGR
CyF3'H2	DVVVASSAAA	ASQFLRTHDA	NFSSRPPNSG	AEHVAYNYQD	LVFAPYGARW	RMLRRLCVSH	LFSAKAMEDF	RHVRGGEVER
ChF3'H	DAIVISSASA	AAKCFRSHDA	ILTSRPPNSV	GKYITYNFED	LIMAPYGPRW	QMLRKVCSTH	LLSTKALDSF	RHVWDEDVAM
	* : * .** :	** : : * : **	.***. . .	: : : * * . *	** : * * * . *	: * * * : *	: * : * . * : : .	* : * : *
CyF3'H1	FVRELVKEE-	KFVDSLSDGIS	ACAADALSRV	VVGKRVFGDG	EE---SREFK	EMVMEMMNL	SAFNINDFVP	GLGWLDVQGL
CyF3'H2	LVHGIAEEEG	VAVDVGGAVN	TCTTNALTQV	TVGRRVFGGR	EEKEGAEFEK	EMVVELMNL	GVFNFGDFVP	GLGWLDLQGV
ChF3'H	DVRELTSGRE	AAVDVGGLVN	TCVTNALAHV	LIGRQEIVGG	EE---AAEFK	EIAAEMTTLA	GQFNVGHFIP	WIGWLDLQDL
	* : . . . .	* * . . . .	: * . : * * : *	: * : : . .	** : * * *	* . : * : *	. * * . . * * *	: * * * * . : *
CyF3'H1	VAKMKLHRK	FDEFLDKVI	DHKARLTETE	NATTAAGG	RGRHNDLLSV	LIEAKGDANG	DGIALTDADI	KPLLQNMFAA
CyF3'H2	VRKMKLHRK	FDKLFDFGII	EHRESVEKGD	-----VHG	RG--SDMLS	LLRLKKEADG	EGNLLTDTNI	KALLLNLFAA
ChF3'H	NKKMMKSRVR	FGEFLEKIE	EHSS-----	-----KG	IDYAKDFLSV	LIQINGEPNA	KDELTNINI	KALLQDMFIA
	* * * : : *	* . : : : * :	* :		* . . * * * :	* : . : : . .	. * * : * *	* . * * : * *
CyF3'H1	<b>GTDTS</b> SNTIE	FAIAELIRHP	ELLVRAQOEL	DSVVGRRRLV	AESDLPNLFP	FQAVVKETFR	HHPAAPLSLP	RIISEDYEID
CyF3'H2	<b>GTDTS</b> SSTVE	WAMAELIRHP	NLLKQAQTEL	DSVVGHNRLV	SESDLPNLPF	LQAIVKETFR	LHPSTPLSLP	RVASSDCEID
ChF3'H	<b>GTDTS</b> SITIE	WLLSELLRHP	HILARAQHEL	DSVAGRNRLI	SQSDLPKVPF	LDAIVKETLR	LHPPVPLSVP	RMATEDCEID
	*** : * * *	: : * * * * *	. * : * * *	*** . : * * :	: : * * * * * *	: : * * * * * *	* * . * * * *	* : . * * *
CyF3'H1	GYLIPKGATL	LINIWAIGRD	PIAWADETLA	FQPDRFLPGG	RHEGADVKG-	NDFELIPFGG	GRRICAGMNL	GLRMVQLLSA
CyF3'H2	GHLIPRGATL	LVNVWSIGRD	PSMWPDEPLA	FRPGRFLAGG	RHEGVDVKG-	NDFELIPFGA	GRRICVGLSL	GLRMVQFMFTA
ChF3'H	GYLIPKGAYL	LVNIWAIGRD	LATWHDHPNE	FDPDRFVPGS	PHEADVKGI	NNFELIPFGA	GRRRCAGTKL	GIRVMHFVTA
	* : * * * * *	* * : * * * * *	* * : .	* * * * : *	* * . * * * *	* : * * * * * *	* * * . * * *	* : * * * * : * *
CyF3'H1	TLVHAFDWKL	PEGELPEKLD	MDLSFGLTLH	RTNPLMIRPV	PRLEPEAYV-	--		
CyF3'H2	TLIHAFDWEL	AGGETAEKLD	MEEAYGLTLR	RAAPLVAKPT	TRLALKAYPK	HV		
ChF3'H	MMLHAFDWTL	PDGSMGDLLD	MEEASYGATMP	KTRPLMAKAT	PRLAPQAYL-	--		
	: : * * * * *	* . * . : * * *	* : * * * :	: : * * : . .	. * * : * *			

Supplemental Figure S6



Supplemental Figure S7



**Supplemental Table S1 Primer sequence used in ORF amplification**

	Sequences (5'→3')	
	Forward	Reverse
<i>CyMYB1</i>	ATGAAGAAGAAGCCATTCTGTGACG	TTAAAAATTCATCCAAATATCTGTCTCC
<i>CybHLH1</i>	ATGGCGGTAGATATGCAGAGCCAAGAAG	TTAACATTTGCTGACGGCTCTCTG
<i>CybHLH2</i>	ATGCAGACCCAAGAGGAGCTGCAG	TTAACATTTGCTGACGGCTCTCTG
<i>CyCHI</i>	CGACATGGCAGAAACGCCGGCAAC	TCAAGCGACCTCAACTTGCTCGAAC
<i>CyEFP</i>	ATGAGTTCGAAAGAGGTGATGATAG	CTATTTTGACAATATTGCTTCAAATTTCTC
<i>CyF3H</i>	ATGGCGCCAGTACAATTCCTCCCCAC	TTAAGCTAGAATTCGTTTAATGTC
<i>CyF3'H1</i>	ATGGCCATTCTCTCCCTCCTCCTCGTAC	TCAAACATAAGCCTCCGGTTCAAGCCGG
<i>CyF3'H2</i>	ATGGCTCTCGTAATCTTCGTCCTCTTCG	TTAGACATGCTTAGGATATGCCTTTAGG
<i>CyANS</i>	ATGGCCACCAGAACCATCCCCGCTAC	TCACGACCCGTGCTCCTGCTTCCTC
<i>Cy3GT</i>	ATGGTCCTCTCTAGCGATTCATCTCCGC	TCAATTTCTGCAAACCAACGCCACCAG
<i>Cy3RT</i>	ATGGCCAACAACGATGAAGTTACGGCC	TCACTTGGATGATTTATCATAAGCCAA
<i>CyMalT</i>	ATGGCATCTTTAAGAATACTCG	TCAAGCCCACCTAGTAAGAAAC
<i>CyFLS</i>	ATGGAGGTGGAAATACAGAGAGTCCAATC	TCACTGCGGCAGCTTGTTGATTTTGCAG

**Supplemental Table S2 Primer sequence used in qRT-PCR analysis**

Sequences (5'→3')		
	Forward	Reverse
<i>CyMYB1</i>	GAGCCAAAATTA AAAACCTCAAGAA	CATTGATTCATCTCCAAAGTTCTG
<i>CybHLH1</i>	TACCCAGATATTGCAGAAAGAACA	TGGCTTCAATTATGTCAAGGAGTA
<i>CybHLH2</i>	CATCAATAGACTGAATGAGCCATC	CTTCCTCAATTCCTAAAGAACCAA
<i>CyCHS</i>	CCGGACTACTACTTCAGAATCACA	TCAGAATCTCTTCCGTTAGGTACA
<i>CyCHI</i>	CCGAGACATAATTACAGGTTCCCT	GAATGAGTGAAGATGATGGAAGTG
<i>CyEFP</i>	GAAGAAGGATTCTGTGATCACCTT	GCATTCTCCACTTGGATCTTACTT
<i>CyF3H</i>	CGTGAAGCTCTAACCCAAGC	CTGAACGGTGATCCAGGTTT
<i>CyF3'H1</i>	ATTTGATGAATTTTTGGACAAGGT	TTCGCTTCTATCAGCACACTTAAC
<i>CyF3'H2</i>	TGAAGAAGCTGCATAAAAAGATTTG	TCAGTAAGAGAGCCTTGATGTTTG
<i>CyDFR</i>	GAAAGCTTCGACGAGGTGAC	GGTGTTCCTCCACGTTCACT
<i>CyANS</i>	GATTCAGGGCTATGGAAGCA	TCCTCAGCAAAAAGAGGTCGT
<i>Cy3GT</i>	TTCGGCGATTCTAACTCTAAATTC	AACTGAAGAGAGTTCATGGGAGTC
<i>Cy3RT</i>	AAGCTAGTGCTGTTACCGCTTAGA	CATCCAAGAAAACTCTCTCCACT
<i>CyMalT</i>	CCTACTCTCCGCCATGGAAATAGA	CGATTGTGGAGATTGGAGATGATG
<i>CyFLS</i>	AGGATAAGTATGCGATGAAGGAAG	CCCTCTAGAAAGCCACTTCAATAG
<i>CyACT1</i>	TTGTTAGGGACATAAAGGAGAAGC	ATTCATGATGGAGTTGTATGTGG